Author's Proof

Accumulation of Environmental Insults

An interesting report has established the significance of the accumulation of environmental insults such as viruses and chemicals (Toniolo et al. 1980). The concept may also be applicable to type 2 diabetes, where accumulation of risk factors such as diet, obesity, aging, genetic risk, and little exercise together lead to impaired insulin action, resulting in the development of diabetes. Viral infection may contribute to the development of type 2 diabetes when viral infection alone is not sufficient to induce diabetes, but the damage to β-cells may reduce β-cell function to some extent. In this sense, viral infection may serve as another risk factor for the development of type 2 diabetes, although direct evidence is lacking.

Autoimmunity

The EMC virus is a cytolytic virus but does not cause persistent infection, and therefore infected cells are not likely to be attacked by cytotoxic T cells similar to the autoimmune reaction. However, infiltration of T cells with a restricted T-cell receptor repertoire has been reported, suggesting a pathogen and/or autoantigen-directed reaction (Kawagishi et al. 2003). Indeed, lysed cells after infection with the EMC virus would release self-antigens and thus may possibly trigger autoimmunity to pancreatic β-cells as well as virus antigen-directed protective immune response (Flodström et al. 2002; Christen et al. 2010). The hit-and-run theory is hard to confirm and/or disclaim with evidence for or against paradigm. In addition, interferon production induced by viral infection may play a role in the development of autoreactivity to pancreatic β-cells (Fig. 5.4) (Devendra and Eisenbarth 2004). Recent advances in controlling organ-specific autoimmune diseases often associated with autoimmune type 1 diabetes, the significance of AIRE being in the thymus and Treg in the peripheral immunoregulation system have been extensively described in addition to microbial environment engagement (Nagamine et al. 1997; Kogawa et al.2002; Eisenbarth and Gottlieb 2004; Sakaguchi 2005). Programmed death factor, suppressor of cytokine signaling (SOCS), and B lymphocytes may also contribute to the prevention of autoimmunity to pancreatic β-cells (Chervonsky 2010; Yoshimura, et al. 2007; Pescovitz et al. 2009; Nagafuchi et al. 2010).

[AU6]

Long-Term Complications

Susceptible mice infected with diabetogenic EMC-D virus develop hyperglycemia and develop characteristic diabetic complications similar to those in humans such as glomerulosclerosis, retinal vessel involvement, and decrease in bone formation and mineralization. The diabetic mice with glomerulosclerosis after 6 months' duration

Author's Proof

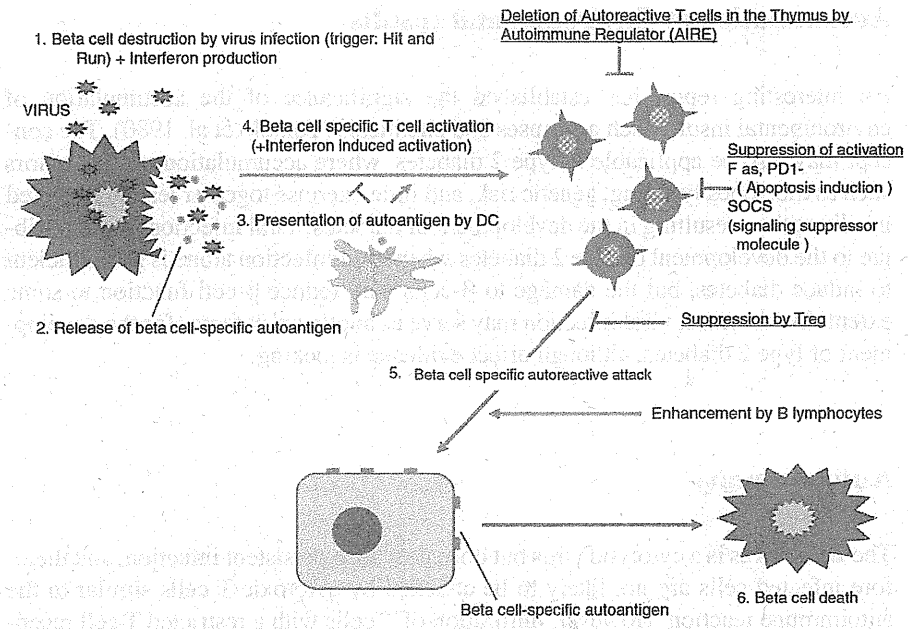

Fig. 5.4 Hypothesis: possible induction of autoreactivity to pancreatic β cells triggered by viral infection

revealed the two- to threefold increase in thickness of the glomerular basement membrane. Thickening of Bowman's capsule and the renal mesangial matrix has also been observed in EMC-M virus-infected DBA/2 mice 2–6 months after infection (Yoon et al. 1982).

Host Factors

Even diabetogenic EMC-D virus induced diabetes only in a few strains of mice such as SJL/J, SWR, DBA/1J, DBA/2J, while others such as C57BL/6, CBA/J, AKR, C3H/HeJ. A/J mice are all resistant to EMC-D virus-induced diabetes (Ross et al. 1975; Yoon et al. 1980; Huber et al. 1985). Onodera and others have reported that F1 hybrid mice between susceptible SWR and resistant C57BL/6 mice were resistant to virus-induced diabetes, while the next F1 and SWR mating showed that 50% of those mice exhibited the susceptibility to the virus, thus indicating that a single autosomal recessive gene, which is inherited in a Mendelian fashion, controls the susceptibility to the virus (Onodera et al. 1978). It was indicated that the susceptibility gene may modulate the expression of virus receptors on β-cells in susceptible mice (Kang and Yoon 1993); however the exact controlling gene has remain to be identified.

Author's Proof

Prevention

Several preventive strategies have been reported to be effective. As described in the pathogenesis section, Nitrate oxide inhibitors and chemokine suppression may reduce the diabetogenic effect of EMC virus infection. Since the antibody is very effective to prevent the EMC virus infection, vaccination and every early phase of the disease may be effective in preventing the EMC virus-induced diabetes (Kounoue et al. 2008). Immunostimulants such as BCG, *Corynebacterium parvum*, and PolyIC treatment have been shown to be effective in preventing EMD-D virus-induced diabetes (Kounoue et al. 1987; Choi et al. 2000).

Perspectives

EMC virus has contributed greatly to better understanding of the pathogenesis of virus-induced diabetes. The data described above show the development of diabetes even under the diabetogenic virus challenge, with the outcome being influenced by many factors, such as genetic background, sex, protective immunity, inflammatory cells, cytotoxic mediators, and also perhaps the regenerative activity of pancreatic β-cells (Hover and Sauter 2010). The elevation of blood glucose level may be due to the accumulation of such "risk factors," leading to the development of virus-induced diabetes. Moreover, since even susceptible strains of inbred mice develop virus-induced diabetes in a rather variable but not homogeneous fashion, the "stochastic process" in this model and/or human virus-induced diabetes should therefore be recognized. In order to acquire a better understanding of the pathogenesis of virus-induced diabetes, the assay system for the diabetogenicity of the virus together with clarification of host genetic risk factors should be exploited, as these may lead to the identification of the "diabetogenic" virus. Those studies will hopefully lead to the development of a vaccination strategy to the "diabetogenic" virus, which will in turn not only prevent the development of the virus-induced type 1 diabetes but may also contribute to reduce the risk for the development of type 2 diabetes.

Summary

- EMC virus has provided the most useful animal model for virus-induced type 1 diabetes. Development of diabetes depends on many factors including virus strain, challenge dose, host factors such as genetic background, sex, immunoprotective function, inflammatory responses with macrophages, cytokines, chemokines, and chemical mediators.
- Autoimmunity induction is not likely to be a factor in this model, though a hit-and-run event cannot be excluded.

Author's Proof

- Most importantly, the difference between the diabetogenic strain D (EMC-D) and the non-diabetogenic strain B (EMC-B) virus depends on only one amino acid change due to single point mutation of "A" to "G" at position 3155 (Thr-776 to Ala-776), suggesting that possible acquisition of diabetogenicity may occur often among environmental "non-diabetogenic" viruses.
- Although susceptibility to the EMC-D virus-induced diabetes depends on the genetic background of mice, the genetic determinants of the host remain to be elucidated.

Clarification of the pathogenesis of EMC virus-induced diabetes will not only promote a better understanding of the mechanisms of virus-induced diabetes in general, but will also contribute to the development of new protective strategies against viral diabetes.

Acknowledgments The authors thank Professor Takehiko Sasazuki for his helpful advice. We also thank Dr. Chiri Nagatsuka and Mrs Arisa Moroishi for their help in the preparation of the manuscript. Financial support by Ministry of Health, Labour and Welfare of Japan is acknowledged.

References

Bae YS, Eun HM, Yoon JW (1989) Genomic differences between the diabetogenic and non-diabetogenic variants of encephalomyocarditis virus. Virology 170:282–287

Bae Y, Yoon JW (1993) Determination of diabetogenicity attributable to a single amino acid Ala776, on the polyprotein of encephalomyocarditis virus. Diabetes 42:435–443

Baek HS, Yoon JW (1990) Role of macrophages in the pathogenesis of encephalomyocarditis virus-induced diabetes in mice. J Virol 64:5708–5715

Baek HS, Yoon JW (1991) Direct involvement of macrophages in destruction of β-cells leading to development of diabetes in virus-infected mice. Diabetes 40:1586–1597

Choi BK, Cho SH, Bai GH, Kim SJ, Hyun BH, Choe YK, Bae YS (2000) Prevention of encephalomyocarditis virus-induced diabetes by live recombinant mycobacterium bovis Bacillus Calmette-Guerin in susceptible mice. Diabetes 49:1459–1467

Chervonsky AV (2010) Influence of microbial environment on autoimmunity. Nat Immunol 11:28–33

Christen U, Hintermann E, Holdener M, von Herrath MG (2010) Viral triggers for autoimmunity: is the 'glass of molecular mimicry' half full or half empty? J Autoimmun 34:38–44

Clements GB, Galbraith DN, Taylor KW (1995) Coxsackie B virus infection and onset of child hood diabetes. Lancet 346:221–223

Craighead JE, McLane MF (1968) Diabetes mellitus induction in mice by encephalomyocarditis virus. Science 162:913–914

Devendra D, Eisenbarth GS (2004) Interferon alpha—a potential link in the pathogenesis of viral-induced type 1 diabetes and autoimmunity. Clin Immunol 111:225–233

Eisenbarth GS, Gottlieb PA (2004) Autoimmune polyendocrine syndromes. N Engl J Med 350:2068–2079

Eun HM, Bae Y, Yoon JW (1988) Amino acid differences in capsid protein, VP1, between diabetogenic and nondiabetogenic variants of encephalomyocarditis virus. Virology 163:369–373

Fehsel AK, Jalowy A, Qi S, Burkart V, Hartmann B, Kolb H (1993) Islet cell DNA is a target of inflammatory attack by nitric oxide. Diabetes 42:496–500

Author's Proof

Flodström M, Maday A, Balakrishna D, Cleary MM, Yoshimura A, Sarvetnick N (2002) Target cell defense prevents the development of diabetes after viral infection. Nat Immunol 3:373–382

Hanafusa T, Imagawa A (2008) Insulitis in human type 1 diabetes. Ann NY Acad Sci 1150:297–299

Hirasawa K, Ogiso Y, Takeda M, Lee MJ, Itagaki S, Doi K (1995) Protective effects of macrophage-derived interferon against encephalomyocarditis virus-induced diabetes mellitus in mice. Lab Anim Sci 45:652–656

Hirasawa K, Jun HS, Maeda K, Kawaguchi Y, Itagaki S, Mikami T, Baek HS, Doi K, Yoon JW (1997) Possible role of macrophage-derived soluble mediators in the pathogenesis of encephalomyocarditis virus-induced diabetes in mice. J Virol 71:4024–4031

Hover D, Sauter P (2010) Pathogenesis of type 1 diabetes mellitus: interplay between enterovirus and host. Nat Rev Endocrinol 6:279–289

Huber SA, Babu PG, Craighead JE (1985) Genetic influences on the immunologic pathogenesis of encephalomyocarditis (EMC) virus-induced diabetes mellitus. Diabetes 34:1186–1190

Jenson AB, Rosenberg HS, Notkins AL (1980) Pancreatic islet-cell damage in children with fatal viral infections. Lancet 316:354–358

Jun HS, Kang Y, Notkins AL, Yoon JW (1997) Gain or loss of diabetogenicity result in from a single point mutation in recombinant encephalomyocarditis virus. J Virol 71:9782–9785

Jun HS, Kang Y, Yoon HS, Kim KH, Notkins AL, Yoon JW (1998) Determination of encephalomyocarditis viral diabetogenicity by a putative binding site of the viral capsid protein. Diabetes 47:576–582

Jun HS, Yoon JW (2001) The role of viruses in type I diabetes: two distinct cellular and molecular pathogenic mechanisms of virus-induced diabetes in animals. Diabetologia 44:271–285

Kang Y, Yoon JW (1993) A genetically determined host factor controlling susceptibility to encephalomyocarditis virus-induce diabetes in mice. J Gen Virol 74:1207–1213

Kaptur PE, Thomas DC, Giron DJ (1989) The role of interferon in the protection of ICR Swiss male mice by the nondiabetogenic variant of encephalomyocarditis virus against virus-induced diabetes mellitus. J Interferon Res 9:671–678

Kawagishi A, Kubosaki A, Takeyama N, Sakudo A, Saeki K, Matsumoto Y, Hayashi T, Onodera T (2003) Analysis of T-cell receptor Vβ gene from infiltrating T cells in insulitis and myocarditis in encephalomyocarditis virus-infected BALB/C mice. Biochem Biophys Res Commun 310:791–795

Kogawa K, Kudoh J, Nagafuchi S, Ohga S, Katsuta H, Ishibashi H, Harada M, Hara T, Shimizu N (2002) Distinct clinical phenotype and immunoreactivity in Japanese siblings with autoimmune polyglandular syndrome type 1 (APS-1) associates with compound heterozygous novel AIRE gene mutations. Clin Immunol 103:277–283

Kounoue E, Nagafuchi S, Nakamura M, Nakano S, Koga T, Nakayama M, Mitsuyama M, Niho Y, Takaki R (1987) Encephalomyocarditis (EMC) virus-induced diabetes mellitus prevented by Corynebacterium parvum in mice. Experientia 43:430–431

Kounoue E, Izumi K, Ogawa S, Kondo S, Katsuta H, Akashi T, Niho Y, Harada M, Tamiya S, Kurisaki H, Nagafuchi S (2008) The significance of T cells, B cells, antibodies, and macrophages against encephalomyocarditis (EMC)-D virus-induced diabetes in mice. Arch Virol 153:1223–1231

McCartney SA, Vermi W, Lonardi S, Rossini C, Otero K, Calderon B, Gilfillan S, Diamond MS, Unanue ER, Colonna M (2011) RNA sensor-induced type I IFN prevents diabetes caused by a β-cell tropic virus in mice. J Clin Invest 121:1497–1507

Nagafuchi S, Katsuta H, Anzai K (2010) Rituximab, B-lymphocyte depletion, and beta-cell function. N Engl J Med 362:761

Nagamine K, Peterson P, Scott HD, Kudoh J, Minoshima S, Heino M, Krohn KJE, Lalioti MD, Mullis PE, Antonarakis SE, Kawasaki K, Asakawa S, Ito F, Shimizu N (1997) Positional cloning of the APECD gene. Nat Genet 17:393–398

Onodera AT, Yoon JW, Brown ES, Notkins AL (1978) Evidence for a single locus controlling susceptibility to virus-induced diabetes mellitus. Nature 274:693–696

Author's Proof

338 Pescovitz MD, Greenbaum CJ, Krause-Steinrauf H, Becker DJ, Gitelman SE, Goland R, Gottlieb
339 PA, Marks JB, McGee PF, Moran AM, Raskin P, Rodriguez H, Schatz DA, Wherrett D, Wilson
340 DM, Lachin JM, Skyler JS (2009) Rituximab, B-lymphocyte depletion, and preservation of
341 beta-cell function. N Engl J Med 361:2143–2152
342 Rabinovitch A, Suarez-Pinzon WL, Shi Y, Morgan AR, Bleackley RC (1994) DNA fragmentation
343 is an early event in cytokine-induced islet beta-cell destruction. Diabetologia 37:733–738
344 Racaniello VR (2007) Picornaviridae: the viruses and their replication. In: Knipe DM, Howley
345 PM, Griffin DE, Lamb RA, Straus SE, Martin MA, Roizman B (eds) Fields virology, 5th edn.
346 Lippincott Williams & Wilkins, Philadelphia, pp 795–838
347 Richardson AJ, Willcox A, Bone AJ, Morgan N, Foulis AK (2011) Immunopathology of the human
348 pancreas in type-I diabetes. Semin Immunopathol 33:9–21
349 Ross ME, Onodera T, Brown KS, Notkins AL (1975) Virus-induced diabetes mellitus. IV. Genetic
350 and environmental factors influencing the development of diabetes after infection with the M
351 variant of encephalomyocarditis virus. Diabetes 25:190–197
352 Sakaguchi S (2005) Naturally arising Foxp3-expressiong $CD25^+$ $CD4^+$ regulatory T cells in immu-
353 nological tolerance to self and non-self. Nat Immunol 6:345–398
354 Santos CX, Anjos EI, Augusto O (1999) Uric acid oxidation by peroxynitrate: multiple reaction,
355 free radical formation, and amplification of lipid oxidation. Arch Biochem Biophys
356 372:285–294
357 Smyth DJ, Cooper JD, Bailey R, Field S, Burren O, Smink LJ, Guja C, Ionescu-Tirgoviste C,
358 Widmer B, Dunger DB, Savage DA, Walker NM, Clayton DG, Todd JA (2006) A genome-wide
359 association study of nonsynonymous SNPs identifies a type 1 diabetes locus in the interferon-
360 induced helicase (IFIH1) region. Nat Genet 38:617–619
361 Takeuchi O, Akira S (2009) Innate immunity to virus infection. Immunol Rev 227:75–86
362 Tanaka S, Nishida Y, Aida K, Maruyama T, Shimada A, Suzuki M, Shimura H, Takizawa S,
363 Takahashi M, Akiyama D, Arai-Yamashita S, Furuya F, Kawaguchi A, Kaneshige M, Katoh R,
364 Endo T, Kobayashi T (2009) Enterovirus infection CXC chemokine ligand 10 (CXCL10), and
365 CXCR3 circuit. Diabetes 58:2285–2291
366 Tauriainen S, Oikarinen S, Oikarinen M, Hyöty H (2011) Enteroviruses in the pathogenesis of type
367 1 diabetes. Semin Immunopathol 33:45–55
368 Toniolo A, Onodear T, Yoon JW, Notkins AL (1980) Induction of cumulative environmental insults
369 from viruses and chemicals. Nature 288:383–385
370 Yamamoto H, Uchigata Y, Okamoto H (1981) Streptozocin and alloxan induced DNA strand
371 breaks and poly ADP-ribose synthetase in pancreatic islets. Nature 294:284–286
372 Yoon JW, McLintock PR, Onodera T, Notkins AL (1980) Virus-induced diabetes mellitus. XVIII.
373 Inhibition by a nondiabetogenic variant of encephalomyocariditis virus. J Exp Med
374 152:878–892
375 Yoon JW, Rodrigues MM, Currier C, Notkins AL (1982) Long-term complications of virus-induced
376 diabetes mellitus in mice. Nature 296:566–569
377 Yoon JW, McClintock PR, Bachurski CJ, Longstreth JD, Notkins AL (1985) Virus-induced diabe-
378 tes mellitus. No evidence for immune mechanisms in the destruction of β-cell by the D-variant
379 of encephalomyocarditis virus. Diabetes 34:922–923
380 Yoshimura A, Naka T, Kubo M (2007) SOCS proteins, cytokine signaling and immune regulation.
381 Nat Rev Immunol 7:454–465

From bloodjournal.hematologylibrary.org at CENTRAL LIBRARY (M080) on May 21, 2012. For personal use only.

R723, a selective JAK2 inhibitor, effectively treats JAK2V617F-induced murine myeloproliferative neoplasm

*Kotaro Shide,[1] Takuro Kameda,[1] *Vadim Markovtsov,[2] Haruko K. Shimoda,[1] Elizabeth Tonkin,[2] Shuling Fang,[2] Chian Liu,[2] Marina Gelman,[2] Wayne Lang,[2] Jason Romero,[2] John McLaughlin,[2] Somasekhar Bhamidipati,[2] Jeffrey Clough,[2] Caroline Low,[2] Andrea Reitsma,[2] Stacey Siu,[2] Polly Pine,[2] Gary Park,[2] Allan Torneros,[2] Matt Duan,[2] Rajinder Singh,[2] Donald G. Payan,[2] Takuya Matsunaga,[1] Yasumichi Hitoshi,[2] and Kazuya Shimoda[1]

[1]Department of Gastroenterology and Hematology, Faculty of Medicine, Miyazaki University, Kiyotake, Miyazaki, Japan, and [2]Rigel Pharmaceuticals Inc, San Francisco, CA

The activating mutations in JAK2 (including *JAK2V617F*) that have been described in patients with myeloproliferative neoplasms (MPNs) are linked directly to MPN pathogenesis. We developed R723, an orally bioavailable small molecule that inhibits JAK2 activity in vitro by 50% at a concentration of 2nM, while having minimal effects on JAK3, TYK2, and JAK1 activity. R723 inhibited cytokine-independent CFU-E growth and constitutive activation of STAT5 in primary hematopoietic cells expressing JAK2V617F. In an anemia mouse model induced by phenylhydrazine, R723 inhibited erythropoiesis. In a leukemia mouse model using Ba/F3 cells expressing JAK2V617F, R723 treatment prolonged survival and decreased tumor burden. In V617F-transgenic mice that closely mimic human primary myelofibrosis, R723 treatment improved survival, hepatosplenomegaly, leukocytosis, and thrombocytosis. R723 preferentially targeted the JAK2-dependent pathway rather than the JAK1- and JAK3-dependent pathways in vivo, and its effects on T and B lymphocytes were mild compared with its effects on myeloid cells. Our preclinical data indicate that R723 has a favorable safety profile and the potential to become an efficacious treatment for patients with *JAK2V617F*-positive MPNs. (*Blood*. 2011;117(25):6866-6875)

Introduction

Myeloproliferative neoplasms (MPNs) are clonal hematologic diseases characterized by excess production of one or more lineages of mature blood cells, resulting in a predisposition to bleeding and thrombosis, extramedullary hematopoiesis (EMH), and a progression to acute leukemia.[1] A somatic activating mutation encoding a valine to phenylalanine substitution at position 617 (V617F) in JAK2 was discovered as a common molecular marker in Philadelphia chromosome–negative MPNs.[2-5] The incidence of the *JAK2V617F* mutation is found in > 90% of patients with polycythemia vera (PV) and affects approximately half of the patients with essential thrombocythemia (ET) and primary myelofibrosis (PMF). Expression of JAK2V617F in vivo in a murine BM transplantation assay resulted in erythrocytosis resembling PV.[6-8] Moreover, we and others have reported that JAK2V617F-transgenic (V617F-TG) mice develop 3 kinds of MPNs: PV like, ET like, and PMF like.[9-11] These studies support a critical role for JAK2V617F in the pathogenesis of the 3 types of MPNs.

Current therapy for MPNs[12-14] is empirically derived and includes phlebotomy,[15] hydroxyurea,[16] IFN-α,[17] anagrelide,[16] and thalidomide[18] and its analogs.[19] Most patients are not candidates for stem-cell transplantation, which is the curative treatment for MPNs,[20] given their advanced age at the time of diagnosis, considerably high ratio of transplantation-related mortality, and relatively indolent progression. Identification of specific JAK2 inhibitors appears to be an important step toward the development of targeted therapy for MPNs. Several groups of investigators have begun to develop specific, potent, orally bioavailable JAK2 inhibitors for the treatment of MPNs,[21-24] and these compounds are currently undergoing clinical trials.[25-27]

In the present study, we report the development of R723, a selective small-molecule JAK2 inhibitor. We show that R723 is a potent inhibitor of JAK2V617F in cell-based assays. In 3 mouse models, R723 had significant in vivo activity against JAK2V617F, was well tolerated, and had a minimal impact on T- and B-cell numbers.

Methods

Materials

Cell lines, the JAK2V617F clone, and vectors are described in supplemental Methods (available on the *Blood* Web site; see the Supplemental Materials link at the top of the online article).

Identification of JAK2 inhibitors

To identify JAK2 inhibitors, we used a cell-based approach using murine leukemia Ba/F3 cells expressing JAK2V617F with the erythropoietin (EPO) receptor Ba/F3-EPOR-JAK2V617F. Initially, we screened a focused, diversified kinase inhibitor library to identify inhibitors of Ba/F3-EPOR-JAK2V617F cell proliferation. To avoid nonselective compounds targeting other members of the JAK family and molecules with general toxicity, we

Submitted January 3, 2010; accepted April 15, 2011. Prepublished online as *Blood* First Edition paper, April 29, 2011; DOI 10.1182/blood-2010-01-262535.

*K.S. and V.M. contributed equally to this study.

The online version of this article contains a data supplement.

The publication costs of this article were defrayed in part by page charge payment. Therefore, and solely to indicate this fact, this article is hereby marked "advertisement" in accordance with 18 USC section 1734.

© 2011 by The American Society of Hematology

From bloodjournal.hematologylibrary.org at CENTRAL LIBRARY (M080) on May 21, 2012. For personal use only.

used 2 additional assays assessing the effects on IL-2–dependent proliferation of human primary T lymphocytes, CTLL-2 mouse T-cell leukemia cells, and JAK1-dependent Ba/F3 cells expressing JAK1V658F. The use of these counterscreen assays also allowed us to exclude the possibility of cell-type- and species-specific artifacts. R723 was obtained as a result of the systemic chemical modification of the initial hits, followed by testing of the resulting compounds in the assays mentioned above.

In vitro proliferation assays

The half-maximal inhibitory concentration (IC_{50}) for the inhibition of proliferation of all the cell lines was determined using CellTiter-Glo Luminescent Cell Viability Assay reagent (Promega). For details, see supplemental Methods.

Cell-based STAT5 phosphorylation assay

Effects of R723 on STAT5 phosphorylation in human primary T cells and cell lines were determined by FACS. For details, see supplemental Methods.

Animals

Eight-week-old female BALB/c mice and 7-week-old female NOD/SCID mice (The Jackson Laboratory) were used in the induced hemolytic anemia model and PK-PD studies and in the Ba/F3-JAK2V617F leukemia study, respectively. Two lines of V617F-TG mice were established and analyzed as described previously.[9] In this experiment, we used line 2 mice that showed the spectrum of clinicopathologic features of human PMF.[9] Animal studies were performed in the United States in accordance with the Institutional Animal Care and Use Committee of Rigel Pharmaceuticals Inc, and in Japan in accordance with the Miyazaki University Ethics Committee.

Analysis of JAK2- and JAK1/JAK3-dependent STAT5 phosphorylation in primary cells

Wild-type (WT) mice (female BALB/c) were dosed orally with R723 at 50 or 100 mg/kg or vehicle, and blood was collected at 1 and 3 hours after treatment. After stimulation with either 10 ng/mL of GM-CSF for the assessment of JAK2 activity in granulocytes (Gr-1$^+$) or 100 ng/mL of IL-15 for the assessment of JAK1/JAK3 activity in T cells (CD8$^+$), the cells were fixed and permeabilized and then stained with Alexa Fluor 647–conjugated pSTAT5 and either PE-conjugated Gr-1 or peridinin chlorophyll A protein–cyanin 5.5–conjugated CD8. Samples were analyzed by FACS.

PHZ-induced hemolytic anemia model and Ba/F3-JAK2V617F engraftment mouse model

Phenylhydrazine (PHZ; Sigma-Aldrich) was administered at 50 mg/kg/d intraperitoneally for 2 consecutive days to deplete RBCs and to stimulate erythropoiesis. R723 formulated in 0.1% hydroxypropyl methylcellulose was administered by oral gavage starting the day after the final PHZ administration (day 2). R723 dosing continued through day 7 at 50 mg/kg or 75 mg/kg twice daily. Blood was collected on days 3, 6, and 8 to assess RBC number and hematocrit levels. The Ba/F3-JAK2V617F engraftment mouse model is described in supplemental Methods.

Murine MPN model and analysis of mice after R723 treatment

Twelve-week-old V617F-TG mice were treated by oral gavage twice daily with 35 mg/kg R723, 70 mg/kg R723, or vehicle for 16 weeks. In this study, a salt form of R723 was formulated in water to ease the formulation process. As a control for V617F-TG treated with vehicle, we prepared WT mice treated with vehicle. Differential blood counts were assessed by retro-orbital eye bleeds before study initiation, during the study, and at the end of the study. Mice were killed at the study end point. For pathologic examination, tissue samples were fixed in formalin, embedded in paraffin blocks, and sectioned for H&E staining or Gomori silver staining. FACS was performed as described previously.[9]

V617F-TG BM cell engraftment mouse model

BM cells (2 to 8 × 10^6) from CD45.2$^+$ V617F-TG mice, together with 2 × 10^5 CD45.1$^+$ WT BM cells, were injected into 9.5 Gy–irradiated recipient CD45.2$^+$ WT mice. In our preliminary experiments, we injected 2 × 10^6 CD45.1 BM cells into lethally irradiated (9.5 Gy) CD45.2 recipients. Reconstitution of recipients with donor BM cells was monitored by assessing the frequency of CD45.1$^+$/CD45.2$^+$ cells in the peripheral blood (PB) after transplantation. Twelve weeks after the transplantation, donor-derived (CD45.1) cells had nearly completely replaced (99%) the recipient (CD45.2) cells in the PB. The remaining recipient cells in PB were 1%. Therefore, under the conditions of our cotransplantation experiments, nearly all of the CD45.2$^+$ cells in the PB were derived from V617F-TG. Twenty weeks after BM transplantation, recipient mice were divided into R723 treatment or vehicle control groups. R723 was administered by oral gavage at 70 mg/kg twice daily for 4 weeks, whereas the control group received vehicle only. Complete blood counts and the ratio of CD45.1$^+$ to CD45.2$^-$ cells were monitored by FACS before and after treatment. All mice were killed at study end points and spleens were weighed.

Progenitor cell assays

Colony forming assays were performed as described previously[9] (for details, see supplemental Methods). CFU-E colonies were counted on day 3 and other colonies were counted on day 7. To observe the effect of R723 on the proportion of progenitors, V617F-TG mice were dosed orally with R723 at 70 mg/kg or vehicle twice daily for 4 weeks. Lin$^-$Sca-1$^-$cKit$^+$ (LSK), common myeloid progenitor (CMP), granulocyte-macrophage progenitor (GMP), erythromegakaryocyte progenitor (MEP), megakaryocyte progenitor (MKP), early erythroblast, and late erythroblast populations in BM cells were determined by FACS. Antibodies were used as indicated in supplemental Methods.

Statistical analysis

Results are presented as means ± SE. To assess the statistical significance between the 2 groups, the 2-tailed Student t test was used. Statistical analyses of R723-treated groups versus vehicle groups in survival studies were performed with the log-rank test.

Results

R723 is a potent selective JAK2 inhibitor

To identify JAK2 inhibitors, we used a cell-based approach using murine leukemia Ba/F3 cells expressing JAK2V617F with the EPO receptor Ba/F3-EPOR-JAK2V617F. R723 was obtained as a potent and selective inhibitor of Ba/F3-EPOR-JAK2V617F proliferation through a screening of a focused, diversified kinase inhibitor library and through the structure-activity relationship study on the initial hits from the screening. The chemical structure of R723 and the crystal structure of R723 complexed with JAK2 catalytic domain are shown in supplemental Figure 1 (US Patent Application Pub. No. 2009-0258864 A1, October 15, 2009). R723 strongly suppressed proliferation of Ba/F3-EPOR-JAK2V617F and 2 other cell lines dependent solely on JAK2V617F signaling for survival: UKE-1 and SET-2.[28] R723 strongly diminished JAK2-dependent STAT5 phosphorylation in these cells (Table 1 and supplemental Figure 2A). R723 potently targeted WT JAK2 activity, as indicated by the inhibition of EPO-driven proliferation of human CD34$^+$-derived erythroid progenitors. We then compared the ability of R723 to inhibit WT JAK2-dependent proliferation of Ba/F3-EPOR cells in the presence of EPO with that of JAK2V617F-dependent (and cytokine-independent) proliferation of Ba/F3-EPOR-JAK2V617F cells. Both cell lines were inhibited equally well by the compound, showing the lack of R723 selectivity between WT

From bloodjournal.hematologylibrary.org at CENTRAL LIBRARY (M080) on May 21, 2012. For personal use only.

Table 1. R723 activity in cell-based assays

Assay	Target	IC_{50}, nM
Ba/F3-EPOR-JAK2V617F proliferation	JAK2 V617F	191
UKE1 proliferation	JAK2 V617F	168
SET2 proliferation	JAK2 V617F	139
EPO-dependent human CD34+ progenitor proliferation	JAK2	124
Ba/F3-EPOR-JAK2V617F pSTAT5 FACS	JAK2 V617F	390
SET2 pSTAT5 FACS	JAK2 V617F	39
IL-2 CTLL2 proliferation	JAK1/JAK3	528
IL-2 human primary T-cell proliferation	JAK1/JAK3	1260
IL-2 CTLL2 pSTAT5 FACS	JAK1/JAK3	2300
IL-2 human primary T-cell pSTAT5 FACS	JAK1/JAK3	2700
Ba/F3-JAK1V658F proliferation	JAK1 V658F	885
CMK proliferation	JAK3 A572V	2340
A549 proliferation	Multiple	3680
H1299 proliferation	Multiple	4100
IgE CHMC tryptase	Syk	760
Insulin HeLa pAKT in cell western	InsR	10 800
VEGF HUVEC pVEGFR in cell western	VEGFR	3250

and mutant forms of the enzyme in cells (supplemental Figure 2B). This observation agrees with the in vitro kinase inhibition data, in which no differences between the 2 were found (supplemental Table 1).

Characterization of R723 included a variety of cell-based assays probing multiple pathways (summarized in Table 1). The effects of R723 on the key off-target assays, IL-2–dependent proliferation and STAT5 phosphorylation via JAK1/JAK3 in human primary T lymphocytes and CTLL-2 cells, were significantly lower than the effects observed in the JAK2-dependent cell lines (Table 1). We also used a Ba/F3 cell line expressing the V658F mutant of JAK1 kinase (Ba/F3-JAK1V658F cells), which demonstrates IL3-independent but JAK1-dependent growth,[29] and the CMK cell line, which is dependent on the constitutively active JAK3A572V mutant, for survival and proliferation assays.[30] Both cell lines were weakly affected by R723. We observed moderate inhibition of Syk kinase activity, leading to a suppression of IgE-stimulated tryptase release in human mast cells. This effect, however, became pronounced only at a concentration higher than the one required for efficient inhibition of the JAK2-dependent pathway.

Biochemical selectivity of R723

As expected from the results of the cell-based assays, R723 was shown to be an extremely potent JAK2 inhibitor, with a biochemical IC_{50} of 2nM (Table 2). It had a nearly identical inhibition profile for both the WT and the V617F mutant of JAK2 in a 2-point in vitro kinase assay (supplemental Table 1). R723 demonstrated good selectivity against all other JAK family kinases when tested at a wide range of concentrations. Selectivity ratios for IC_{50} varied from 13-fold for JAK3 to a few hundred–fold for 2 other members of the family, JAK1 and Tyk2 (Table 2). The R723 selectivity was further confirmed by 2-point testing against a full panel of more than 200 enzymes. Only 13 other kinases cleared a threshold of 30% inhibition at 100nM, with the majority of them failing to show any discernable inhibition at 20nM, a concentration that is 10-fold higher than the JAK2 IC_{50} (supplemental Table 1). These results indicate that R723 is a highly potent and selective JAK2 inhibitor in vitro.

Table 2. R723 selectively inhibits JAK2

Kinase	IC_{50}, nM	Selectivity over JAK2, -fold
JAK2	2	NA
JAK1	740	370
JAK3	26	13
TYK2	3950	> 500
VEGFR2	1400	> 500
Syk	300	150
PKCa	3960	> 500
PKCb1	7990	> 500
PKCd	> 10 000	> 500
PKCe	> 10 000	> 500
PKCq	> 10 000	> 500
PLK1	> 10 000	> 500
RET	109	55

R723 demonstrates selectivity in primary cells

R723 is an orally bioavailable compound demonstrating excellent pharmacokinetic properties in mice, making it a good candidate for in vivo testing (supplemental Figure 3). To assess the effects of R723 on JAK2 and JAK1/JAK3 signaling in vivo, we measured STAT5 phosphorylation in whole blood obtained from R723-treated WT mice (female BALB/c) on ex vivo stimulation of either Gr-1+ granulocytes with GM-CSF or CD8+ T cells with IL-15, respectively. Whereas the GM-CSF–mediated signaling cascade relied exclusively on JAK2, IL-15–dependent stimulation of T cells required both JAK1 and JAK3 activities. Both 50 and 100 mg/kg doses of R723 induced strong inhibition of STAT5 phosphorylation after GM-CSF and, to a lesser extent, IL-15 stimulation, especially when a 50 mg/kg dose of R723 was administered (Figure 1A). We consistently observed a preference for targeting the JAK2-dependent GM-CSF pathway, especially at the 50 mg/kg dose 1 hour after dosing.

R723 inhibits erythropoiesis in a PHZ-induced hemolytic anemia model

To investigate the ability of R723 to inhibit JAK2 in vivo, we used the acute mouse model based on induction of anemia on PHZ treatment.[31] PHZ-induced RBC damage and sequential depletion lead to hyperstimulation of normal and EMH accompanied by transient splenomegaly, followed by quick (7-10 days) recovery to normal hematocrit levels. As expected, 3 days after the first PHZ injection, both hematocrit and RBC values in all groups dropped to an average of 66% and 64% of naive controls, respectively. On days 6 and 8, however, progressive recovery was observed in vehicle control animals, whereas animals administered R723 showed a dose-dependent and significant ($P < .05$) delay in recovery (Figure 1B), with the 75 mg/kg twice daily dose producing the strongest effect on both parameters ($P < .01$).

R723 is effective in an acute Ba/F3-JAK2V617F leukemia model

We investigated the effect of R723 in a mouse leukemia model relying on the use of murine Ba/F3 cells expressing JAK2V617F as a driver of cell proliferation. This model is particularly aggressive, with a lethal outcome within 15 days of cell injection in vehicle-treated mice. In the R723-treated group, we observed a small (2 days, 13%) but highly significant improvement in survival ($P < .004$) compared with the vehicle-treated cohort (supplemental Figure 4). In another study, animals were killed on day 13, before the full disease onset, to evaluate the levels of green fluorescent protein–positive (GFP+) Ba/F3-JAK2V617F cells in the spleen and BM. We observed a significant decrease in spleen cellularity and in

From bloodjournal.hematologylibrary.org at CENTRAL LIBRARY (M080) on May 21, 2012. For personal use only.

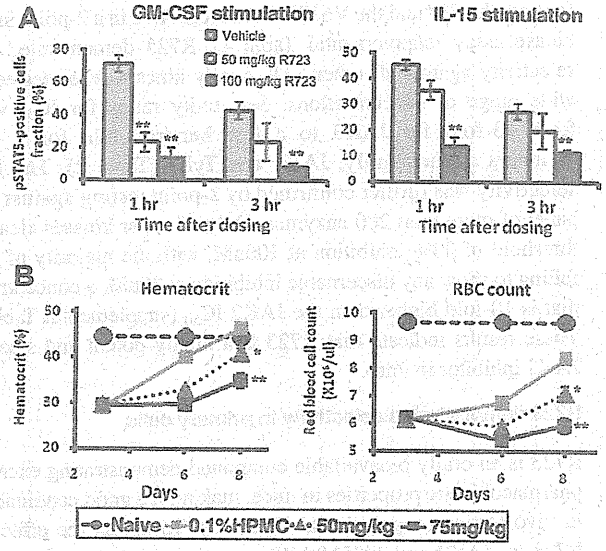

Figure 1. R723 shows selectivity and efficacy in mice. (A) Analysis of JAK2- and JAK1/JAK3-dependent STAT5 phosphorylation in primary cells. WT mice (female BALB/c) were orally dosed with vehicle, R723 50 mg/kg, or R723 100 mg/kg. Blood was collected at 1 and 3 hours after dosing and stimulated with either GM-CSF or IL-15. The percentage of pSTAT5-positive Gr-1$^+$ cells with GM-CSF stimulation (left panel) and the percentage of pSTAT5-positive CD8$^+$ cells with IL-15 stimulation (right panel) at each time point are shown. (B) R723 is efficacious in the hemolytic anemia mouse model. Hematocrit (left panel) and RBC count (right panel) changes were examined in mice administered PHZ on days 0 and 1 followed by oral daily administration of R723 or vehicle on days 2-7. Hematocrit and RBC counts of naive mice on day 3 were used as a baseline. (C) NOD/SCID mice injected with Ba/F3-JAK2V617F cells were administered with saline, vehicle (hydroxypropyl methylcellulose), or 50 mg/kg of R723 twice daily. Spleens and BM were harvested 13 days after cell injection. Cell counts per spleen (left panel) and percentage of GFP$^+$ cells (Ba/F3-JAK2V617F) in BM and spleen cells (right panel) are shown. Data are presented as means ± SE. $^{**}P < .01$; $^{*}P < .05$.

GFP$^+$ cells in BM and spleen from R723-treated mice compared with those from untreated or vehicle-treated mice (Figure 1C).

In vitro growth inhibition of JAK2V617F-harboring hematopoietic cells by R723

We investigated the effect of R723 in a murine model of MPN induced by JAK2V617F. $H2K_b$ promoter–controlled JAK2V617F-expressing mice (V617F-TG) show extreme leukocytosis, thrombocytosis, and progressive anemia,[9] as well as hepatosplenomegaly with EMH, megakaryocytosis, and fibrosis in the BM. BM cells show constitutive activation of STAT5 and formation of cytokine-independent growth of CFU-E colonies (as is also seen in JAK2V617F-positive MPN patients) and exhibit high mortality compared with WT mice. These features of V617F-TG closely resemble PMF patients and their progression.

We also investigated the in vitro efficacy of R723 on WT and V617F-TG BM cells by assessing STAT5 activation in Mac-1/Gr-1$^+$ cells. Cells were starved of growth factors for 4 hours and then stimulated with IL-3, EPO, and G-CSF. V617F-TG myeloid cells had more phosphorylated basal levels of STAT5 than WT myeloid cells, and after IL-3 + EPO + G-CSF stimulation, the degree of phosphorylation further increased. In vitro treatment of V617F-TG myeloid cells with R723 resulted in a marked decrease in phosphorylation of STAT5 (Figure 2A). These data indicate that R723 is capable of inhibiting activation of STAT5, the main effector of JAK-STAT signaling, in primary hematopoietic cells expressing JAK2V617F.

We next assessed the effect of R723 on EPO-independent colony formation. R723 inhibited EPO-independent CFU-E growth of BM cells from V617F-TG in a dose-dependent manner. A 5-fold reduction at 800nM R723 was observed (Figure 2B). Cytokine-dependent colony formation (CFU-E, CFU-GEMM, CFU-GM, and BFU-E) was also inhibited by the presence of R723. In all colony types, R723 inhibited colony growth of both V617F-TG and WT cells at the same level (Figure 2C). This agrees reasonably well with the results of a 2-point in vitro kinase assay in which R723 showed an identical inhibition profile for both WT and the V617F mutant of JAK2 (supplemental Table 1).

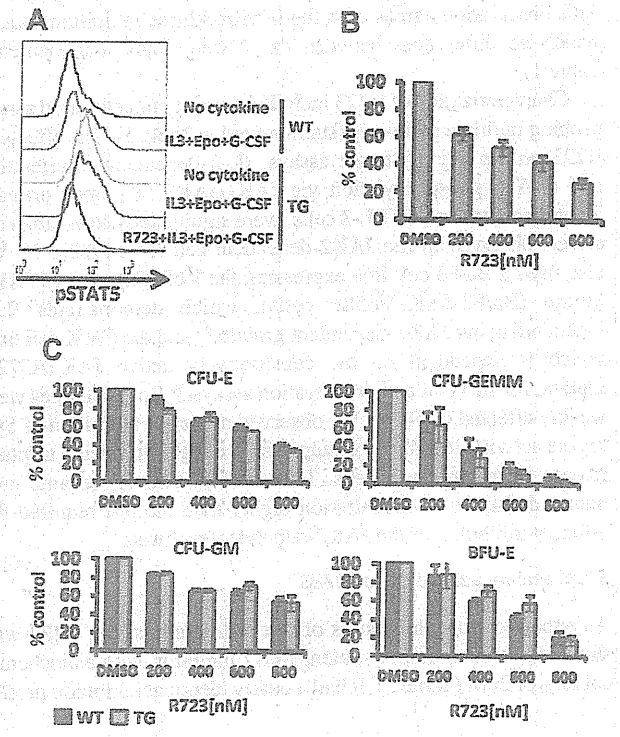

Figure 2. R723 inhibits JAK/STAT signaling and growth of JAK2V617F harboring hematopoietic cells. (A) BM cells from WT or V617F-TG mice were harvested and cultured without serum for 3 hours. Cells were incubated with vehicle or R723 for 1 hour, followed by the stimulation with IL-3, EPO, and G-CSF for 15 minutes. Mac-1/Gr-1$^+$ myeloid cells were analyzed for levels of STAT5 phosphorylation by flow cytometry. One representative experiment of 3 is shown. (B) Effects of R723 on EPO-independent CFU-E colonies derived from V617F-TG. BM cells from V617F-TG were cultured in duplicate in methylcellulose culture medium in the absence of EPO with and without R723. The number of CFU-E colonies was counted on day 3. R723 treatment significantly suppressed CFU-E in V617F-TG. Three independent experiments were performed. Data are presented as means ± SE. (C) Effects of R723 on cytokine-dependent BM colonies derived from WT and V617F-TG mice. BM cells from WT and V617F-TG mice were cultured in cytokine-containing methylcellulose with and without R723. The number of CFU-E colonies was counted on day 3 (top left). The numbers of CFU-GEMM (top right), CFU-GM (bottom left), and BFU-E (bottom right) colonies were counted on day 7. R723 inhibited the cytokine-dependent colonies (CFU-E, CFU-GEMM, CFU-GM, and BFU-E) derived from both WT and V617F-TG cells to the same extent. Three independent experiments were performed, each using 1 different WT mouse and 1 different V617F-TG mouse. Data are presented as means ± SE.

From bloodjournal.hematologylibrary.org at CENTRAL LIBRARY (M080) on May 21, 2012. For personal use only.

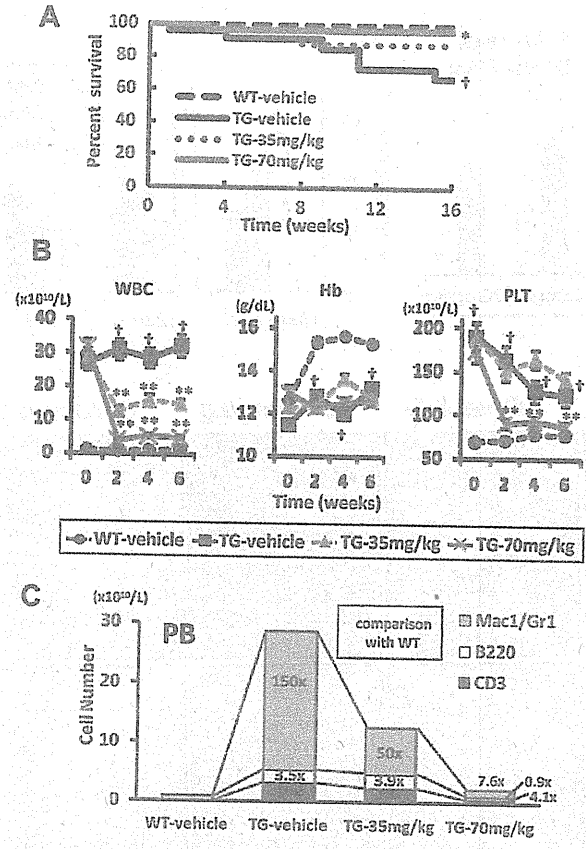

Figure 3. Survival and changes of PB of V617F-TG mice treated with R723. (A) Kaplan-Meier plot of WT mice treated with vehicle (WT-vehicle) and V617F-TG mice treated with vehicle (TG-vehicle), 35 mg/kg of R723 (TG-35mg/kg), or 70 mg/kg of R723 (TG-70mg/kg) for 16 weeks. There was a statistical difference in survival between the TG-vehicle group and the WT-vehicle group (†$P < .01$) and between the TG-70mg/kg group and the TG-vehicle group (*$P < .05$ by log-rank test). (B) Differential blood counts in WT-vehicle and TG-vehicle, TG-35mg/kg, or TG-70mg/kg treated with R723 for 6 weeks. V617F-TG mice showed severe leukocytosis and thrombocytosis at 12 weeks of age compared with age-matched WT mice (†$P < .01$). The leukocyte and platelet count in V617F-TG mice treated with R723 was significantly reduced compared with the TG-vehicle group (**$P < .01$). V617F-TG mice had anemia (†$P < .01$) that was not improved by R723 treatment. Data are presented as means ± SE. (C) Hematopoietic compartment of PB assessed by flow cytometry. At 18 weeks of age in the TG-vehicle group, the Mac-1/Gr-1$^+$ myeloid cells were significantly increased in number and the B220$^+$ B cells and CD3$^-$ T cells were increased to a lesser extent than myeloid cells. R723 treatment for 6 weeks significantly decreased the number of Mac-1/Gr-1$^+$ myeloid cells ($P < .01$) and mildly decreased the number of B220$^+$ B cells and CD3$^+$ T cells ($P < .05$). Data are means of 6 mice in each group.

R723 effectively improves survival, leukocytosis, and EMH in JAK2V617F-induced murine MPN

At 12 weeks of age, all V617F-TG mice developed MPN exhibiting leukocytosis, with average white blood cell counts of 29 × 10^{10}/L. V617F-TG mice were divided into 3 groups and treated with R723 by oral gavage at 35 mg/kg twice daily (TG-35mg/kg; n = 30), 70 mg/kg twice daily (TG-70mg/kg; n = 26), or vehicle twice daily (TG-vehicle; n = 23) for 16 weeks. As a control for TG-vehicle, we prepared WT mice treated with vehicle (WT-vehicle; n = 30). During the study, 6 of 23 in the TG-vehicle group and 3 of 30 in the TG-35mg/kg group died, whereas only 1 of 26 mice in the TG-70mg/kg group died (Figure 3A). Therefore, administration of R723 at 70 mg/kg twice daily significantly improved the survival of V617F-TG mice ($P < .05$).

V617F-TG mice at 12 weeks of age had severe leukocytosis (Figure 3B). After 2 weeks of R723 treatment, the leukocyte count was reduced to 45% in the TG-35mg/kg group ($P < .01$) and to 13% in the TG-70mg/kg group ($P < .01$) compared with the TG-vehicle group, and the effect was maintained until the end of the study (Figure 3B). In V617F-TG mice, not only Mac-1/Gr-1 myeloid cells, but also B220$^+$ B cells and CD3$^+$ T cells increased in number. Compared with the numbers in WT, the numbers of myeloid cells, B cells, and T cells were increased by 150-fold, 3.5-fold, and 19-fold, respectively (Figure 3C). After 6 weeks of 70 mg/kg R723 treatment in V617F-TG mice, the number of PB myeloid cells, B cells, and T cells reached 7.6-fold, 0.9-fold, and 4.1-fold, respectively, compared with that in WT (Figure 3C). Although R723 treatment reduced the number of all types of PB cells in a dose-dependent manner, the reduction of myeloid cell number was the most significant ($P < .01$): to less than one-tenth of that of the TG-vehicle group. A reduction in platelet count of 48% was observed in the TG-70mg/kg group ($P < .01$) compared with the TG-vehicle group (Figure 3B). Because platelet numbers in the TG-vehicle group were reduced gradually in the natural disease course, the difference between the 2 groups disappeared after 9 weeks of treatment. In contrast to the effect on leukocyte and platelet numbers, there was no improvement in anemia in V617F-TG mice treated with R723 (Figure 3B).

R723 treatment also improved hepatosplenomegaly in V617F-TG mice in a dose-dependent manner (Figure 4A). In the spleen, Mac-1/Gr-1$^+$ myeloid cells associated with EMH were significantly decreased, and B220$^+$ B cells were relatively increased by R723 treatment (Figure 4B). Along with reduction of organ weights and infiltrating mycloid cells, there was also clear evidence of a dose-dependent reduction in histopathology of EMH in the spleen, liver, and lungs from R723-treated V617F-TG mice (Figure 4C). Histopathological analysis of spleens from the TG-vehicle group exhibited complete effacement of normal splenic architecture and invasion of myeloid cells, whereas R723 treatment resulted in a marked reduction of cell invasion and restored architecture in V617F-TG spleens. Changes in the liver and lungs were more dramatic. EMH consisting of infiltrates of maturing myeloid cells and megakaryocytes seen in the TG-vehicle group were reduced in a dose-dependent manner by R723 treatment and almost completely disappeared in the TG-70mg/kg group (Figure 4C). In contrast to the drastic pathological improvement in spleen, liver, and lung (Figure 4C), R723 had little effect on the progression of fibrosis and megakaryocyte hyperplasia in BM (data not shown).

We also evaluated the histopathological toxicity of R723 in the brain, heart, kidney, ovary, testes, and gastrointestinal tract. There were no signs of toxicity related to R723 in any tissue examined at either the 35 mg/kg or the 70 mg/kg dose.

Transplantation of BM cells from V617F-TG causes MPN in WT recipient mice. These mice exhibited granulocytosis, splenomegaly, EMH, and mild BM fibrosis. CD45.2$^+$ BM cells from V617F-TG mice were injected into irradiated recipient WT mice, together with CD45.1$^+$ WT BM cells. Twenty weeks after BM transplantation, we administrated R723 or vehicle by oral gavage at 70 mg/kg twice daily for 4 weeks. As shown in Table 3, R723 treatment decreased the number of leukocytes, especially in Mac-1$^+$ or Gr-1$^+$ myeloid cells, in recipient mice. The number of B or T lymphocytes in the PB was not affected by R723 treatment, nor was the hemoglobin value or platelet number. In recipient mice, the number of CD45.2$^+$ V617F-TG-derived cells decreased, whereas CD45.1$^+$ WT-derived cells remained unchanged by R723 treatment, indicating that R723 selectively inhibited cells harboring V617F JAK2. A 5-fold reduction in spleen weights in R723-treated

From bloodjournal.hematologylibrary.org at CENTRAL LIBRARY (M080) on May 21, 2012. For personal use only.

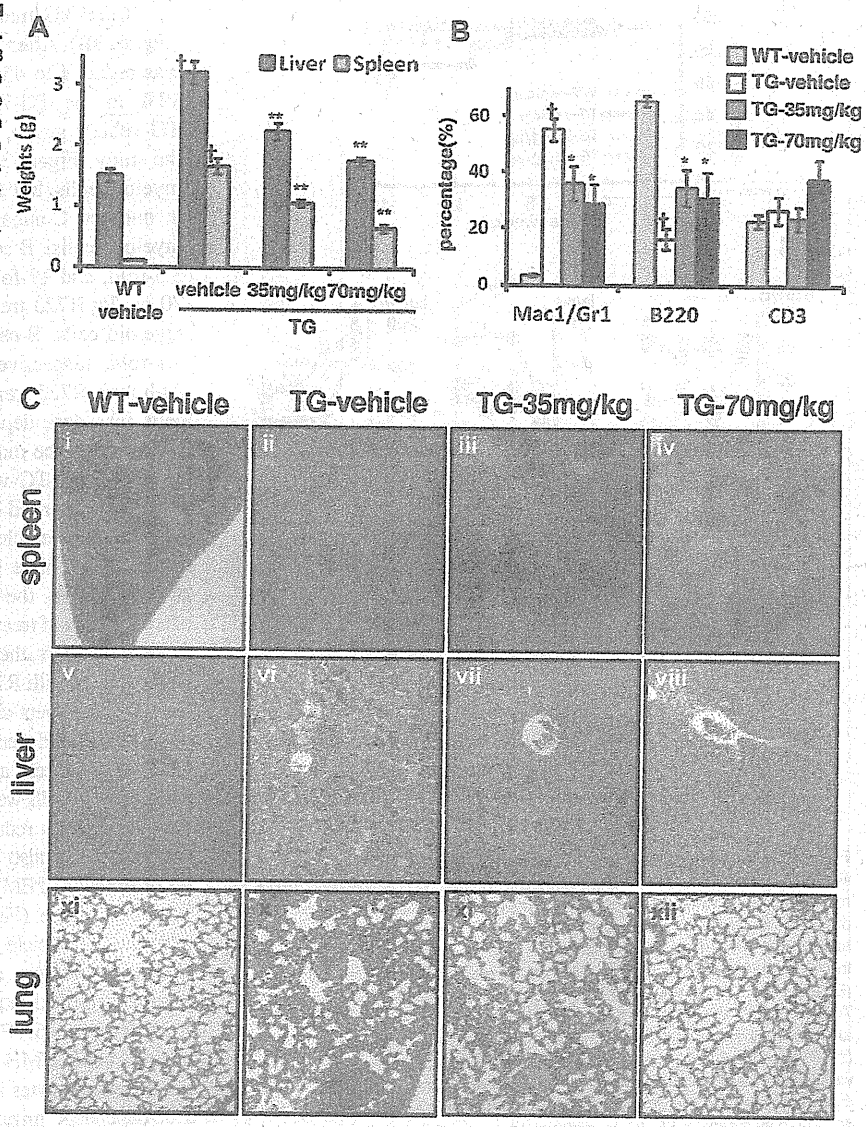

Figure 4. Improvement of hepatosplenomegaly and EMH in V617F-TG mice treated with R723 for 6 weeks. (A) R723 effects on liver and spleen weights after R723 treatment for 6 weeks. Liver and spleen weights in V617F-TG mice treated with vehicle (TG-vehicle) were increased compared with those in WT mice treated with vehicle (WT-vehicle) (†$P < .01$). R723 treatment in V617F-TG mice significantly reduced organ weights (**$P < .01$). Data are presented as means ± SE. (B) Hematopoietic compartment of spleen assessed by FACS. The proportion of Mac-1/Gr-1$^+$ myeloid cells significantly increased, and that of B220$^+$ B cells decreased in 18-week-old TG-vehicle mice compared with age-matched WT-vehicle mice (†$P < .01$). R723 treatment in V617F-TG mice for 6 weeks decreased the proportion of Mac-1/Gr-1$^+$ myeloid cells and increased the proportion of B220$^+$ B cells (*$P < .05$). The percentage of CD3$^+$ T cells was constant. Data are presented as means ± SE. (C) Histological changes in V617F-TG mice by R723 treatment for 6 weeks. Histology of WT-vehicle and V617F-TG mice treated with vehicle, 35 mg/kg, and 70 mg/kg doses of R723 (TG-vehicle, TG-35mg/kg, TG-70mg/kg, respectively). Cells were stained with H&E. In the spleens of the TG-vehicle mice, the red pulp was expanded with maturing myeloid cells and megakaryocytes and the white pulp was scarce compared with WT-vehicle mice (i-ii). Mice treated with R723 for 6 weeks showed marked reduction of myeloid cell invasion and partially restored architecture (iii-iv). Liver and lung sections from TG-vehicle also displayed EMH (vi and x). Infiltration of myeloid cells disappeared with R723 treatment in V617F-TG mice (vii,viii,xi,xii).

recipient mice compared with the vehicle-treated recipient mice was also observed. R723 treatment caused a significant reduction of BM fibrosis (supplemental Figure 5), although the degree of myelofibrosis severity in recipient mice was much milder than that in V617F-TG mice.

The effect of R723 on BM progenitor cells in V617F-TG mice

FACS was performed on BM cells in V617F-TG mice treated with R723 or vehicle. In V617F-TG mice, the proportion of LSK and GMP cells increased ($P < .01$) and the proportions of CMP, MEP,

Table 3. In vivo effect of R723 on JAK2 V617F–harboring cells

	Vehicle (n = 5)		R723 (n = 5)	
	Pretreatment	Posttreatment	Pretreatment	Posttreatment
White blood cells, ×10^3/μL	19.8 (10.8-28.5)	19.8 (10.2-31.8)	15.0 (11.7-25.2)	10.8 (8.1-15.3)*
Mac-1$^+$ or Gr-1$^+$ myeloid, ×10^3/μL	10.7 (3.2-19.2)	11.4 (3.7-22.3)	7.9 (6.4-20.2)	4.6 (3.1-9.2)*
B220$^+$ B cells, ×10^3/μL	2.1 (0.4-9.6)	2.0 (0.4-9.1)	1.9 (0.8-5.1)	2.5 (0.8-3.6)
CD4$^+$ or CD8$^+$ T cells, ×10^3/μL	4.0 (3.0-7.2)	2.8 (2.7-7.5)	4.2 (3.4-4.7)	3.6 (3.1-4.6)
CD45.1$^+$ cells, ×10^3/μL	1.5 (0.8-12.3)	1.6 (0.7-11.2)	1.5 (0.7-8.1)	1.3 (0.7-4.4)
CD45.2$^+$ cells, ×10^3/μL	12.6 (2.6-27.7)	13.0 (2.2-31.1)	11.1 (6.9-24.5)	7.4 (4.3-14.4)*
Hemoglobin, g/dL	11.3 (11.2-13.9)	11.1 (10.7-14)	12.5 (11.2-14.5)	12.9 (10.7-14.3)
Platelets, ×10^{10}/L	61.9 (50.8-81)	53.2 (14-92.5)	70.8 (52-119)	106 (57.2-137)
Spleen weight, g	n.d.	0.20 ± 0.04	n.d.	0.04 ± 0.01†

Peripheral blood data are presented as medians (range). Spleen weights are presented as means ± SE. The paired data between pretreatment and posttreatment were analyzed with a paired 2-tailed *t* test. The comparison of spleen weights between vehicle-treated mice and R723-treated mice were analyzed with a 2-tailed *t* test.

n.d. indicates no data.

*$P < .05$.

†$P < .01$.

From bloodjournal.hematologylibrary.org at CENTRAL LIBRARY (M080) on May 21, 2012. For personal use only.

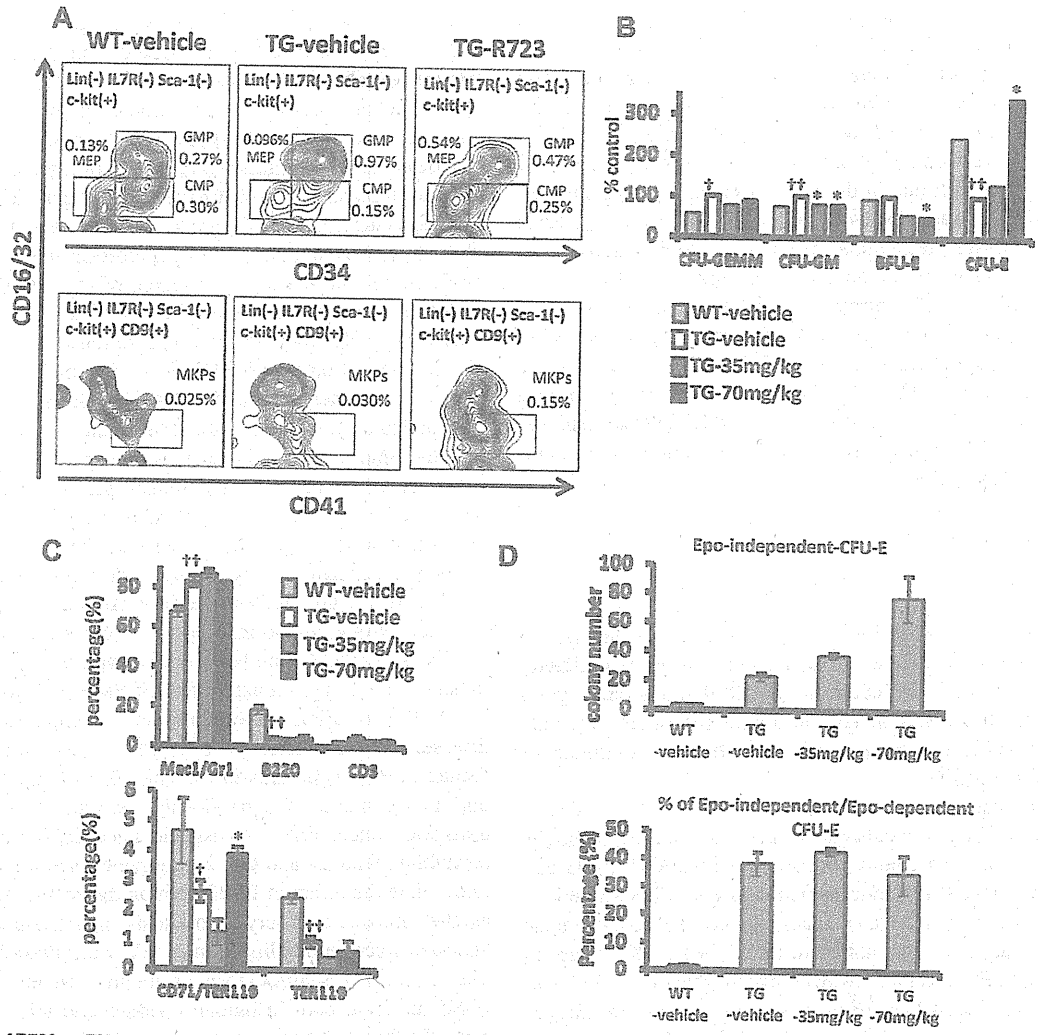

Figure 5. Effect of R723 on BM of V617F-TG mice. (A) BM progenitors in V617F-TG mice and effect of in vivo R723 treatment. V617F-TG mice were dosed orally with R723 at 70 mg/kg or vehicle for 4 weeks. BM cells were collected, and the proportion of CMPs ($Lin^-Sca\text{-}1^-cKit^-CD34^+ Fc\gamma R^{lo}$), GMPs ($Lin^-Sca\text{-}1^-cKit^-CD34^+Fc\gamma R^{hi}$), MEPs ($Lin^-Sca\text{-}1^-cKit^+CD34^-Fc\gamma R^{-/lo}$), and MKPs ($Lin^-cKit^+CD9^+Fc\gamma R^{lo}$ $CD41^+$) was determined by FACS. In V617F-TG mice, the proportion of GMPs increased, and those of CMPs, MEPs, and MKPs were comparable to those in WT mice. Four weeks of R723 treatment in V617F-TG mice normalized the proportion of GMPs. MEPs and MKPs were increased compared with WT mice or V617F-TG mice treated with vehicle. These results are representative of 6 independent experiments. (B) Changes in BM progenitor cells after R723 treatment. The numbers of CFU-GEMM and CFU-GM colonies increased and the numbers of CFU-E colonies decreased in the BM from 18-week-old TG-vehicle mice compared with those in the BM from the age-matched WT-vehicle mice (†$P < .05$; ‡$P < .01$). R723 treatment for 6 weeks suppressed CFU-GM and BFU-E colonies (*$P < .05$). In contrast, CFU-E colonies increased in V617F-TG mice after R723 treatment (**$P < .01$). Data are presented as means ± SE. (C) FACS analysis of BM cells. The percentage of Mac-1/Gr-1$^+$ myeloid cells increased and that of B220$^+$ B cells decreased in 18-week-old V617F-TG mice treated with vehicle (TG-vehicle) compared with the age-matched WT mice treated with vehicle (WT-vehicle) (‡$P < .01$). R723 treatment for 6 weeks had little effect on the proportion of BM myeloid or B cells in V617F-TG mice (top panel). The proportion of CD71/TER119 double-positive erythroblasts and TER119 single-positive erythroblasts decreased in TG-vehicle mice compared with that in WT-vehicle mice (†$P < .05$; ‡$P < .01$). Significant restoration of CD71/TER119-positive erythroblasts was observed in V617F-TG mice after R723 treatment for 6 weeks (*$P < .05$). TER119 single-positive erythroblasts were not restored by R723 treatment (bottom panel). Data are presented as means ± SE. (D) Changes in EPO-independent CFU-E colonies after in vivo R723 treatment. The number of EPO-independent CFU-E colonies increased in BM cells from 18-week-old TG-vehicle mice compared with that in BM cells from the age-matched WT-vehicle mice (†$P < .01$). In vivo R723 treatment for 6 weeks increased the number of EPO-independent CFU-E colonies (*$P < .01$). Data are presented as means ± SE. Whereas EPO-dependent CFU-E colonies increased in V617F-TG mice after in vivo R723 treatment (panel B), the proportion of EPO-independent/EPO-dependent CFU-E colonies remained the same.

and MKP cells were comparable to those of the WT mice. Four weeks of R723 treatment in V617F-TG mice normalized the proportion of GMP cells ($P < .05$). MEP and MKP cells were increased compared with the WT or V617F-TG mice treated with vehicle ($P < .01$; Figure 5A and supplemental Table 2). Conversely, the LSK cell population was not changed by 4 weeks of R723 treatment. The proportion of BM progenitors was also analyzed by colony formation assay. CFU-GEMM and CFU-GM colonies were increased in number in the BM from the TG-vehicle group compared with that from the WT-vehicle group. The suppression of CFU-GM was observed in V617F-TG by R723 treatment (Figure 5B).

Mac-1/Gr-1$^+$ myeloid cells in the BM of the TG-vehicle group were increased, and B220$^+$ B cells were decreased compared with that of the WT-vehicle group (Figure 5C). R723 treatment had little effect on the proportion of BM myeloid and B cells in V617F-TG mice.

We then extended our analysis to erythroid-lineage cells. The proportions of CD71/TER119 double-positive early erythroblasts and TER119 single-positive late erythroblasts were decreased in

From bloodjournal.hematologylibrary.org at CENTRAL LIBRARY (M080) on May 21, 2012. For personal use only.

the TG-vehicle group compared with those in the WT-vehicle group (Figure 5C and supplemental Table 2). Significant restoration of CD71/TER119 double-positive early erythroblasts was observed in the TG-70mg/kg group, but TER119 single-positive late erythroblasts were not restored by R723 treatment. CFU-E colonies were decreased in number in the BM from the TG-vehicle group compared with that in the WT-vehicle group. The suppression of BFU-E was observed in V617F-TG mice by R723 treatment; however, the number of CFU-E colonies increased in the TG-70mg/kg group compared with that in the TG-vehicle group (Figure 5B). The number of EPO-independent CFU-E colonies was increased in the V617F-TG group by in vivo R723 treatment compared with that in the TG-vehicle group (Figure 5D). Whereas the number of EPO-dependent CFU-E colonies was increased in V617F-TG mice by in vivo R723 treatment, the proportion of EPO-independent/EPO-dependent CFU-E colonies remained the same.

Discussion

In the present study, R723, a potent, orally bioavailable JAK2-selective inhibitor, was shown to have significant in vitro activity against JAK2V617F. In addition, R723 demonstrated good efficacy and low toxicity in vivo in 3 animal models. Our data indicate that R723 has the potential for effective treatment of V617F-positive MPNs.

R723 was equipotent against both the WT and the V617F mutant-type of JAK2 in biochemical assays and, correspondingly, R723 equally inhibited colony formation of both V617F-TG and WT BM cells. In the PHZ-induced anemia model, R723 was able to significantly delay EPO-driven hematocrit recovery from chemical insult, indicating its in vivo ability to inhibit WT JAK2 kinase in the context of EPO receptor pathway overstimulation. R723 was also effective in 2 JAK2V617F-driven animal models, the Ba/F3-JAK2V617F leukemia model, and in V617F-TG mice. In the aggressive murine leukemia model using Ba/F3-JAK2V617F cells, R723 had clear beneficial effects on disease progression by suppressing the proliferation of tumor cells, which led to an incremental improvement in survival and a decrease in the overall tumor burden in the spleen and BM, although the blood of the R723-treated mice did not inhibit phosphorylation of STAT5 in Ba/F3-JAK2V617F cells completely, only by 30%-40% (supplemental Figure 4 and 1C). The ultimate confirmation of R723 efficacy came from testing it in V617F-TG mice with features closely resembling those seen with human PMF,[9] which is often poorly controlled with conventional therapy and the most appropriate target of a new therapeutic approach using a JAK2 inhibitor. V617F-TG mice have shorter lives than WT mice. In our study, the animals died suddenly, precluding detailed histopathologic analysis. Among a small cohort of V617F-TG mice in which limited necropsy was performed, subcutaneous and intestinal hemorrhage and gangrenous bowels were observed, which might have been caused by abdominal vessel obstruction. In addition, the bleeding time of V617F-TG mice was extremely prolonged compared with that of WT mice (data not shown). We therefore speculated that the cause of death was thrombosis and/or hemorrhage. Mullally et al[32] and Akada et al[33] also reported that thrombotic events might be the cause of V617F-expressing mice. Oral administration of R723 in V617F-TG mice led to the prolongation of survival and profound improvements in leukocytosis, thrombocytosis, and hepatosplenomegaly. These results raise hope for improvements in the treatment of PMF patients. Conversely, anemia, megakaryocyte hyperplasia, and fibrosis in BM were little affected. The effect of R723 on BM fibrosis varied greatly between models. It was not dissolved in V617F-TG mice during R723 treatment, and instead became just as advanced as it was in V617F-TG mice treated with vehicle. R723 treatment caused a significant reduction of myelofibrosis in recipient mice transplanted with V617F-TG BM cells together with WT BM cells (supplemental Figure 5), but the reason for this is not yet clear. Severe progression of myelofibrosis might be resistant to JAK2 inhibition, because the degree of myelofibrosis severity in recipient mice was much milder than that in V617F-TG mice. Interestingly, this outcome closely resembled the results of human clinical trials of other JAK2 inhibitors, in which the main improvements were limited to rapid decreases in spleen size and normalization of leukocyte count without resolution of fibrosis and only marginal improvements in transfusion dependence.[25,26] R723 also has effects in recipient mice transplanted with BM cells from V617F-TG mice. In this transplantation model, R723 seemed to prefer inhibiting the growth of cells harboring V617F to WT cells, although R723 had a nearly identical inhibition profile for both WT and V617F mutant JAK2 in the in vitro kinase assay and equally inhibited colony formation of both WT and V617F-TG BM cells.

The *JAK2V617F* mutation is observed in the majority of PV patients and in approximately half of PMF patients. The effect of the JAK2 mutation on erythropoiesis differs from disease to disease. PV is characterized by erythrocytosis, whereas the main feature of PMF is progressive anemia. The situation was similar in our mouse model. We previously reported 2 lines of V617F-transgenic mice: line 1 transgenic mice exhibiting PV- or ET-resembling features and line 2 transgenic mice (this line was used to evaluate the effect of R723) exhibiting PMF-like diseases such as BM fibrosis, leukoerythroblastosis, and anemia. *JAK2V617F* knock-in mice resembling human PV were described recently.[32] The reason that erythrocytosis or anemia resulted from the same JAK2 mutation both in human diseases and mice models is not clear. We found that some genes were specifically expressed in line 2 transgenic mice (data not shown), and now characterize their roles. These proteins may cooperate with JAK2V617F to influence erythropoiesis.

The effect of R723 on cell components seems to differ by cell lineage. As mentioned previously, R723 did not improve anemia but did effectively improve leukocytosis and thrombocytosis in V617F-TG mice. The frequency of CFU-E and the CD71/TER119 double-positive cells, which represent late erythroid progenitors and erythroblasts,[34] respectively, decreased in V617F-TG mice compared with WT mice, and R723 treatment elevated these erythroid progenitors to levels nearly equal to that of WT mice. This improvement was probably due to the ability of R723 to inhibit the abnormal JAK2V617F signal. However, TER119 single-positive cells, which represent late erythroblasts, were still low in V617F-TG mice after R723 treatment. The generation of committed erythroid progenitors did not require EPO, but the terminal maturation from CD71/TER119 double-positive cells to TER119 single-positive cells did require EPO,[35] indicating that differentiation depends on JAK2 activation. Because R723 inhibits WT JAK2 as well as JAK2V617F, the inhibition of WT JAK2 by R723 might abrogate the terminal differentiation of erythroblasts to erythrocytes, and this might be the reason that anemia was not improved in V617F-TG mice treated with R723. JAK2V617F-selective inhibitors, which do not inhibit WT JAK2, might overcome this problem.

There are JAK2V617F-positive disease-initiating cells that have long-term, multipotent, and self-renewing activity in the

From bloodjournal.hematologylibrary.org at CENTRAL LIBRARY (M080) on May 21, 2012. For personal use only.

hematopoietic stem cell compartment.[36,37] Mullually et al[32] reported that the *JAK2V617F* mutation had nominal effects on the size or function of the LSK compartment critical for MPN initiation and that the JAK2 inhibitor TG101348 failed to eliminate the MPN-initiating population in *JAK2V617F* knock-in mice, even though the treatment demonstrated histopathological improvement of the erythroid hyperplasia and statistically significant reductions in spleen size. As we found in the present study, the compartment of LSK cells increased in V617F-TG mice and R723 treatment did not suppress them, showing again that the effect of R723 on cell components augmented by JAK2V617F seems to differ by cell lineage. R723 effectively suppresses granulopoiesis induced by JAK2V617F, does not suppress LSK cells expanded by JAK2V617F, and suppresses the abnormal JAK2V617F signals in late erythroid progenitors and erythroblasts and the normal EPO signals in late erythrocytes.

To use a JAK2 inhibitor for the treatment of MPNs, long-term therapy is likely to be required for maintenance of remission, such as in the case of imatinib mesylate for BCR-ABL–positive chronic myeloid leukemia.[36] In addition to the standard toxicities, emphasis should be placed on minimization of activity against other kinases, especially JAK1 or JAK3, to prevent immunosuppression associated with prolonged inhibition of JAK3 and possibly JAK1.[37,38] R723 demonstrated reasonable selectivity in both in vitro kinase- and cell-based assays, although the selectivity was somewhat different between the 2 assay systems. In cell-based assays, a few fold selectivity was observed when using mouse CTLL-2 or human primary T cells compared with related JAK2 assays. A single oral dose of R723 demonstrated a preference for targeting the JAK2-dependent GM-CSF pathway in granulocytes rather than the JAK1- or JAK3-dependent IL-15 pathway in T cells. Six weeks of oral administration of R723 to V617F-TG mice showed that the inhibitory effect of R723 on T or B lymphocytes was much less than that on myeloid cells. These data demonstrate that R723 has a limited immunosuppressive effect and a potentially favorable clinical safety profile. All JAK2 inhibitors currently used in clinical trials inhibit JAK2 potently, but their off-target profiles are variable.[21-24] The clinical implications of the distinct profiles remain to be determined.

In conclusion, we identified a potent inhibitor of JAK2, R723, which showed some selectivity in vitro in biochemical and cell-based assays. R723 demonstrated efficacy in vivo in 3 animal models addressing different aspects of disease progression. In V617F-TG mice, which closely mimic human PMF, R723 significantly improved survival, hepatosplenomegaly, leukocytosis, and thrombocytosis, thus confirming the viability of a targeted therapy approach in managing *JAK2V617F*-positive MPNs. We conclude that R723 could become a viable option available to PMF, PV, and ET patients who develop resistance to conventional therapies.

Acknowledgments

We thank C. Wey, M. Matsushita, T. Shinmori, and K. Tsukura for their technical assistance; Dr N. Lin and Dr T. Kitamura for their critical advice; and Dr J. Diehl and Dr T. Young for critical reading of the manuscript.

This work was supported in part by Grants-in-Aid for Scientific Research (20591137, 21010490, and 20790678) from the Ministry of Education, Science, Sports, and Culture in Japan, and by a Grant-in-Aid from the Tokyo Biochemical Research Foundation, Tokyo, Japan.

Authorship

Contribution: K. Shide and V.M. performed research; V.M., E.T., S.F, C.L., M.G., W.L., J.R., J.M., S.B., J.C., C.L., A.R., S.S., P.P., G.P., A.T., M.D., R.S., D.G.P., and Y.H. contributed to screening and initial characterization of the inhibitor; V.M. and Y.H. guided the screening and initial characterization and wrote the manuscript; T.K., H.K.S., and T.M. analyzed results; and K. Shide and K. Shimoda conceived the research, guided its design, analysis, and interpretation, and wrote the manuscript.

Conflict-of-interest disclosure: V.M., E.T., S.F., C.L., M.G., W.L., J.R., J.M., S.B., J.C., C.L., A.R, S.S., P.P., G.P., A.T., M.D., R.S., D.G.P., and Y.H. are or have been employees of Rigel Pharmaceuticals, Inc. The remaining authors declare no competing financial interests.

Correspondence: Kazuya Shimoda, Department of Gastroenterology and Hematology, Faculty of Medicine, Miyazaki University, 5200 Kihara, Kiyotake, Miyazaki 889-1692, Japan; e-mail: kshimoda@med.miyazaki-u.ac.jp.

References

1. Tefferi A, Vardiman JW. Classification and diagnosis of myeloproliferative neoplasms: the 2008 World Health Organization criteria and point-of-care diagnostic algorithms. *Leukemia.* 2008; 22(1):14-22.
2. Baxter EJ, Scott LM, Campbell PJ, et al. Acquired mutation of the tyrosine kinase JAK2 in human myeloproliferative disorders. *Lancet.* 2005; 365(9464):1054-1061.
3. James C, Ugo V, Le Couedic JP, et al. A unique clonal JAK2 mutation leading to constitutive signalling causes polycythaemia vera. *Nature.* 2005; 434(7037):1144-1148.
4. Kralovics R, Passamonti F, Buser AS, et al. A gain-of-function mutation of JAK2 in myeloproliferative disorders. *N Engl J Med.* 2005;352(17): 1779-1790.
5. Levine RL, Wadleigh M, Cools J, et al. Activating mutation in the tyrosine kinase JAK2 in polycythemia vera, essential thrombocythemia, and myeloid metaplasia with myelofibrosis. *Cancer Cell.* 2005;7(4):387-397.
6. Wernig G, Mercher T, Okabe R, Levine RL, Lee BH, Gilliland DG. Expression of Jak2V617F causes a polycythemia vera-like disease with associated myelofibrosis in a murine bone marrow transplant model. *Blood.* 2006;107(11):4274-4281.
7. Bumm TG, Elsea C, Corbin AS, et al. Characterization of murine JAK2V617F-positive myeloproliferative disease. *Cancer Res.* 2006;66(23): 11156-11165.
8. Lacout C, Pisani DF, Tulliez M, Gachelin FM, Vainchenker W, Villeval JL. JAK2V617F expression in murine hematopoietic cells leads to MPD mimicking human PV with secondary myelofibrosis. *Blood.* 2006;108(5):1652-1660.
9. Shide K, Shimoda HK, Kumano T, et al. Development of ET, primary myelofibrosis and PV in mice expressing JAK2 V617F. *Leukemia.* 2008;22(1): 87-95.
10. Tiedt R, Hao-Shen H, Sobas MA, et al. Ratio of mutant JAK2-V617F to wild-type Jak2 determines the MPD phenotypes in transgenic mice. *Blood.* 2008;111(8):3931-3940.
11. Xing S, Wanting TH, Zhao W, et al. Transgenic expression of JAK2V617F causes myeloproliferative disorders in mice. *Blood.* 2008;111(10):5109-5117.
12. Finazzi G, Barbui T. Evidence and expertise in the management of polycythemia vera and essential thrombocythemia. *Leukemia.* 2008;22(8): 1494-1502.
13. Barbui T, Barosi G, Grossi A, et al. Practice guidelines for the therapy of essential thrombocythemia. A statement from the Italian Society of Hematology, the Italian Society of Experimental Hematology and the Italian Group for Bone Marrow Transplantation. *Haematologica.* 2004;89(2): 215-232.
14. Tefferi A. Myelofibrosis with myeloid metaplasia. *N Engl J Med.* 2000;342(17):1255-1265.
15. Pearson TC, Wetherley-Mein G. Vascular occlusive episodes and venous haematocrit in primary proliferative polycythaemia. *Lancet.* 1978;2(8102): 1219-1222.
16. Harrison CN, Campbell PJ, Buck G, et al. Hydroxyurea compared with anagrelide in high-risk essential thrombocythemia. *N Engl J Med.* 2005; 353(1):33-45.

From bloodjournal.hematologylibrary.org at CENTRAL LIBRARY (M080) on May 21, 2012. For personal use only.

17. Tefferi A, Elliot MA, Yoon SY, et al. Clinical and bone marrow effects of interferon alpha therapy in myelofibrosis with myeloid metaplasia. *Blood.* 2001;97(6):1896.
18. Barosi G, Grossi A, Comotti B, Musto P, Gamba G, Marchetti M. Safety and efficacy of thalidomide in patients with myelofibrosis with myeloid metaplasia. *Br J Haematol.* 2001;114(1):78-83.
19. Tefferi A, Cortes J, Verstovsek S, et al. Lenalidomide therapy in myelofibrosis with myeloid metaplasia. *Blood.* 2006;108(4):1158-1164.
20. Patriarca F, Bacigalupo A, Sperotto A, et al. Allogeneic hematopoietic stem cell transplantation in myelofibrosis: the 20-year experience of the Gruppo Italiano Trapianto di Midollo Osseo (GITMO). *Haematologica.* 2008;93(10):1514-1522.
21. Fridman J, Nussenzveig R, Liu P, et al. Discovery and preclinical characterization of INCB018424, a selective JAK2 inhibitor for the treatment of myeloproliferative disorders [Abstract]. *Blood.* 2007; 110(11):3538.
22. Hexner EO, Serdikoff C, Jan M, et al. Lestaurtinib (CEP701) is a JAK2 inhibitor that suppresses JAK2/STAT5 signaling and the proliferation of primary erythroid cells from patients with myeloproliferative disorders. *Blood.* 2008;111(12): 5663-5671.
23. Wernig G, Kharas MG, Okabe R, et al. Efficacy of TG101348, a selective JAK2 inhibitor, in treatment of a murine model of JAK2V617F-induced polycythemia vera. *Cancer Cell.* 2008;13(4):311-320.
24. Verstovsek S, Pardanani AD, Shah NP, et al. A phase I study of XL019, a selective JAK2 inhibitor, in patients with primary myelofibrosis and post-polycythemia vera/essential thrombocythemia myelofibrosis [abstract]. *Blood.* 2007;110(11): 3543.
25. Verstovsek S, Passamonti F, Rambaldi A, et al. A phase 2 study of INCB018424, an oral, selective JAK1/JAK2 inhibitor, in patients with advanced polycythemia vera (PV) and essential thrombocythemia (ET) refractory to hydroxyurea [abstract]. *Blood.* 2009;114(22):311.
26. Pardanani AD, Gotlib JR, Jamieson C, et al. A phase I evaluation of TG101348, a selective JAK2 inhibitor, in myelofibrosis: clinical response is accompanied by significant reduction in JAK2V617F allele burden [abstract]. *Blood.* 2009; 114(22):755.
27. Santos FP, Kantarjian HM, Jain N, et al. Phase II study of CEP-701, an orally available JAK2 inhibitor, in patients with primary or post polycythemia vera/essential thrombocythemia myelofibrosis. *Blood.* 2010;115(6):1131-1136.
28. Quentmeier H, MacLeod RA, Zaborski M, Drexler HG. JAK2 V617F tyrosine kinase mutation in cell lines derived from myeloproliferative disorders. *Leukemia.* 2006;20(3):471-476.
29. Staerk J, Kallin A, Demoulin JB, Vainchenker W, Constantinescu SN. JAK1 and Tyk2 activation by the homologous polycythemia vera JAK2 V617F mutation: cross-talk with IGF1 receptor. *J Biol Chem.* 2005;280(51):41893-41899.
30. Walters DK, Mercher T, Gu TL, et al. Activating alleles of JAK3 in acute megakaryoblastic leukemia. *Cancer Cell.* 2006;10(1):65-75.
31. Menon MP, Karur V, Bogacheva O, Bogachev O, Cuetara B, Wojchowski DM. Signals for stress erythropoiesis are integrated via an erythropoietin receptor-phosphotyrosine-343-Stat5 axis. *J Clin Invest.* 2006;116(3):683-694.
32. Mullally A, Lane SW, Ball B, et al. Physiological Jak2V617F expression causes a lethal myeloproliferative neoplasm with differential effects on hematopoietic stem and progenitor cells. *Cancer Cell.* 2010;17(6):584-596.
33. Akada H, Yan D, Zou H, Fiering S, Hutchison RE, Mohi MG. Conditional expression of heterozygous or homozygous Jak2V617F from its endogenous promoter induces a polycythemia vera-like disease. *Blood.* 2010;115(17):3589-3597.
34. Shimizu R, Engel JD, Yamamoto M. GATA1-related leukaemias. *Nat Rev Cancer.* 2008;8(4): 279-287.
35. Wu H, Liu X, Jaenisch R, Lodish HF. Generation of committed erythroid BFU-E and CFU-E progenitors does not require erythropoietin or the erythropoietin receptor. *Cell.* 1995;83(1):59-67.
36. Druker BJ, Guilhot F, O'Brien SG, et al. Five-year follow-up of patients receiving imatinib for chronic myeloid leukemia. *N Engl J Med.* 2006;355(23): 2408-2417.
37. Nosaka T, van Deursen JM, Tripp RA, et al. Defective lymphoid development in mice lacking Jak3. *Science.* 1995;270(5237):800-802.
38. Rodig SJ, Meraz MA, White JM, et al. Disruption of the Jak1 gene demonstrates obligatory and nonredundant roles of the Jaks in cytokine-induced biologic responses. *Cell.* 1998;93(3): 373-383.

Involvement of Tyrosine Kinase-2 in Both the IL-12/Th1 and IL-23/Th17 Axes In Vivo

Masayuki Ishizaki,*,† Toshihiko Akimoto,† Ryuta Muromoto,* Mika Yokoyama,† Yuya Ohshiro,* Yuichi Sekine,* Hiroaki Maeda,† Kazuya Shimoda,‡ Kenji Oritani,§ and Tadashi Matsuda*

Tyrosine kinase-2 (Tyk2), a member of the Jak family of kinases, mediates the signals triggered by various cytokines, including type I IFNs, IL-12, and IL-23. In the current study, we investigated the in vivo involvement of Tyk2 in several IL-12/Th1– and IL-23/Th17–mediated models of experimental diseases, including methylated BSA injection-induced footpad thickness, imiquimod-induced psoriasis-like skin inflammation, and dextran sulfate sodium– or 2,4,6-trinitrobenzene sulfonic acid-induced colitis. In these disease models, Tyk2 deficiency influenced the phenotypes in immunity and/or inflammation. Our findings demonstrate a somewhat broader contribution of Tyk2 to immune systems than previously expected and suggest that Tyk2 may represent an important candidate for drug development by targeting both the IL-12/Th1 and IL-23/Th17 axes. *The Journal of Immunology*, **2011, 187: 181–189.**

Various combinations of Jak family members selectively associate with cytokine receptors to transmit signals that are involved in various cellular events (1). In the case of tyrosine kinase-2 (Tyk2), it is activated in response to various cytokines, including IFNs, IL-6, IL-10, IL-12, IL-13, and IL-23 (2–7). However, Tyk2 is dispensable for IL-6– and IL-10–mediated signaling in mice (8, 9). We and other investigators reported that Tyk2 is required for IFN-α/β–mediated signals to suppress hematopoietic cell growth but not for the signals that induce antiviral activities (10, 11). Thus, the involvement of Tyk2 in IFN-α/β–mediated signaling is restricted. In contrast, IL-12–mediated signals, especially those for IFN-γ production by T cells, are highly dependent on Tyk2 (8, 9, 12). Because Tyk2 is recruited to IL-12Rβ1, IL-23–mediated signaling also probably involves Tyk2 (7). Consequently, experiments using Tyk2-deficient cells revealed that different levels of dependence on Tyk2 are evident among several cytokines.

IL-12, whose receptor is associated with Tyk2 and Jak2 and mainly activates the transcription factor STAT4, is the lineage-specific cytokine responsible for Th1 generation (5, 13). Phosphorylation of STAT4, in conjunction with signals derived from TCR-mediated stimuli, induces the expression of T-bet, a master transcriptional regulator of IFN-γ–producing Th1 cells (14). Although IL-23 was initially shown to induce the differentiation of Th17 cells, it is now generally accepted that the differentiation of Th17 cells is dependent on TGF-β and IL-6 and that IL-23 is instead involved in the expansion, maintenance, and functional maturation of Th17 cells (15). IL-17 is now believed to play essential roles in the pathogenesis of chronic inflammatory disorders, as well as in the host defenses against various pathogens (15, 16). It is noteworthy that IL-12 and IL-23 have common features. As heterodimeric cytokines, they share the p40 subunit, and their receptors share the IL-12Rβ1 subunit, which associates with Tyk2. Thus, Tyk2 seems to be indispensable for the IFN-γ/Th1 axis but is also involved in the immune responses mediated by IL-17–producing Th17 cells. Because Th1 and Th17 are both mainly involved in the proinflammatory immune responses that are controlled by Tyk2, mutations leading to loss of function of Tyk2 can be expected to lead to striking immunological phenotypes.

Experimental allergic encephalomyelitis (EAE), which is induced by immunization with myelin Ags or by adoptive transfer of myelin-specific CD4 effector cells, is an animal model of multiple sclerosis (17). Notably, recent studies demonstrated that Th17 cells are responsible for the development of EAE (18). Indeed, IL-23p19– and IL-12/IL-23 p40-deficient mice are resistant to EAE (19, 20). Tyk2-deficient mice also show lower clinical scores and inflamed CNS areas in this model (21). Moreover, the involvement of Tyk2 was confirmed by experiments using mice carrying different Tyk2 polymorphisms (22). B10.D1 mice, which express the Tyk2A allele, are resistant to EAE development and can be compensated by one copy of the Tyk2G allele from B10.Q/Ai mice. In addition to the EAE model, mice carrying Tyk2 polymorphisms exhibit susceptibility in a model for collagen-induced arthritis (CIA) (23). B10.Q/Ai mice are highly susceptible to CIA, whereas B10.D1 mice are resistant. These studies suggested that deficiency of Tyk2 results in defined clinical disorders. Recently, a patient with Tyk2 deficiency was reported (24). The patient experienced increased susceptibility to viral and mycobacterial infections, atopic dermatitis, and elevated IgE levels, thereby exhibiting broader and more profound immunological defects than expected from studies of Tyk2-deficient mice. The different

*Department of Immunology, Graduate School of Pharmaceutical Sciences, Hokkaido University, Sapporo 060-0812, Japan; †Frontier Research Laboratories, Kasai Research & Development Center, Daiichi-Sankyo Co., Ltd., Edogawa-ku, Tokyo 134-8630, Japan; ‡Department of Internal Medicine II, Faculty of Medicine, University of Miyazaki, Kiyotake, Miyazaki 889-1692, Japan; and §Department of Hematology and Oncology, Graduate School of Medicine, Osaka University, Suita, Osaka 565-0871, Japan

Received for publication September 30, 2010. Accepted for publication April 22, 2011.

Address correspondence and reprint requests to Dr. Tadashi Matsuda, Department of Immunology, Graduate School of Pharmaceutical Sciences, Hokkaido University, Kita-Ku Kita 12 Nishi 6, Sapporo 060-0812, Japan. E-mail address: tmatsuda@pharm.hokudai.ac.jp

Abbreviations used in this article: CIA, collagen-induced arthritis; DAI, disease activity index; DSS, dextran sulfate sodium; DTH, delayed-type hypersensitivity; EAE, experimental allergic encephalomyelitis; IMQ, imiquimod; mBSA, methylated BSA; TNBS, 2,4,6-trinitrobenzene sulfonic acid; Treg, regulatory T cell; Tyk2, tyrosine kinase-2.

Copyright © 2011 by The American Association of Immunologists, Inc. 0022-1767/11/$16.00

www.jimmunol.org/cgi/doi/10.4049/jimmunol.1003244

Downloaded from http://jimmunol.org/ at Kyushu Univ 00A Noogakubu Tosho on May 21, 2012

dependencies on Tyk2 between human and mice could arise from species specificity. Alternatively, precise analyses of Tyk2-deficient mice may reveal new aspects of Tyk2 functions in vivo.

In the current study, we investigated the in vivo involvement of Tyk2 in several IL-12/IL-23–dependent models of experimental diseases, namely delayed-type hypersensitivity (DTH), imiquimod (IMQ)-induced psoriasis-like skin inflammation, and dextran sulfate sodium (DSS)- or 2,4,6-trinitrobenzene sulfonic acid (TNBS)-induced colitis. Our results indicated a somewhat broader contribution of Tyk2 to immune systems than previously expected and suggested that Tyk2 may represent an important candidate for drug development by targeting both the IL-12/Th1 and IL-23/Th17 axes.

Materials and Methods

Mice

B10.D1-H2q/SgJ (B10.D1) mice bearing the Tyk2A allele and B10.Q/Ai mice with the Tyk2G allele were purchased from The Jackson Laboratory (Bar Harbor, ME) and Taconic Farms (Germantown, NY), respectively. Gene-targeted Tyk2-deficient mice were backcrossed for at least eight generations onto BALB/c mice (8, 25). Mice were kept under specific pathogen-free conditions and provided with food and water ad libitum. All experiments were performed according to the guidelines of the Institutional Animal Care and Use Committee of Hokkaido University and Daiichi-Sankyo.

Cell proliferation assay and ELISA

The proliferation of viable splenocytes after Con A treatment was measured using a WST-8 assay (Cell Counting Kit-8; Dojindo Laboratories, Kumamoto, Japan) (26). Briefly, 10 μl WST-8 solution was added to the cells in each well and incubated for 3 h. Absorbance was measured at a test wavelength of 450 nm, and IL-2 in culture supernatants was measured by specific ELISA (Abcam, Cambridge, U.K.). To quantify IFN-γ and IL-17 production, splenocytes were stimulated with murine IL-2, IL-12, or IL-23 for 48 h or 72 h, and each culture supernatant was measured by specific ELISA (R&D Systems, Minneapolis, MN), according to the manufacturers' instructions.

Analysis of Th cell differentiation

Wild-type and Tyk2-deficient splenocytes were positively selected based on CD4 expression with Dynabeads $CD4^+$ T cell positive selection (Invitrogen, Carlsbad, CA), and the bead-bound cells were detached using DETACHaBEAD (Invitrogen, Carlsbad, CA). The $CD4^+$ T cells were subsequently separated based on CD62L expression with MACS CD62L MicroBeads and MACS separation columns (Miltenyi Biotec, Auburn, CA). The separated naive $CD4^+CD62L^+$ T cells were activated by plate-bound anti-CD3 and soluble anti-CD28 (BD Pharmingen, San Diego, CA) and cultured in the presence of murine IL-6 (50 ng/ml; PeproTech, Rocky Hill, NJ) and human TGF-β (5 ng/ml; R&D Systems) with murine IL-23 (10 ng/ml; R&D Systems) for Th17 cell, IL-12 (1 ng/ml; PeproTech) for Th1 cell, and TGF-β (5 ng/ml) for regulatory T cell (Treg) differentiation (27). After 3 d in culture, cells were restimulated with PMA and ionomycin for 4 h, followed by addition of GolgiPlug (BD Pharmingen). Cells were permeabilized and fixed with Cytofix/Cytoperm (BD Pharmingen), according to the manufacturer's instructions. Detection of IFN-γ– and IL-17–producing cells was determined by intracellular cytokine staining with anti–IFN-γ–FITC or anti–IL-17–PE (BD Pharmingen). Cells were acquired on a FACSCalibur flow cytometer (BD Biosciences, San Jose, CA) and analyzed using CellQuest (BD Biosciences) and FlowJo (TreeStar, Ashland, OR) software.

DTH responses

Six mice per group were injected s.c. with 250 μg methylated BSA (mBSA) (Sigma-Aldrich, St. Louis, MO) at two sites in the abdomen in a combined total of 100 μl a 1:1 emulsion of CFA (BD Biosciences, San Diego, CA) and saline (28). On day 7 following immunization, the mice were challenged by injection of 50 μl 0.5 mg/ml mBSA in saline into one rear footpad, whereas the other rear footpad received 50 μl PBS. Measurements

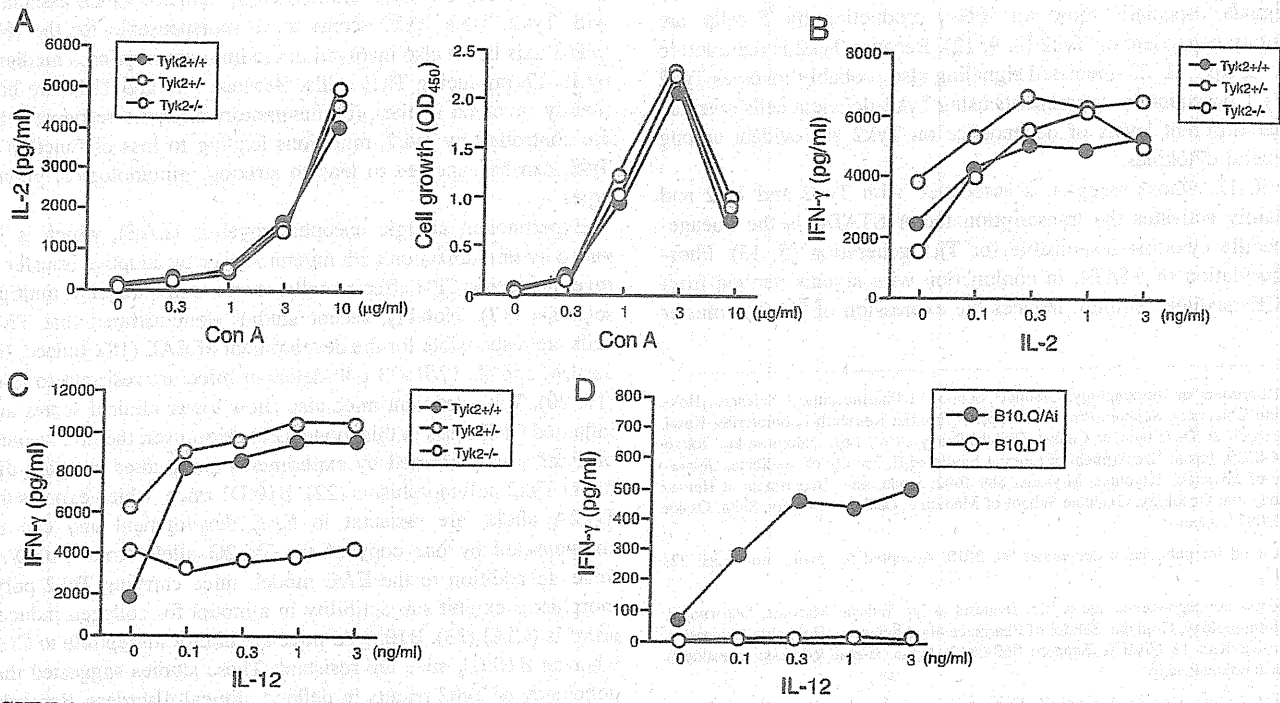

FIGURE 1. Tyk2 is involved in IL-12–induced IFN-γ production and IL-23–induced IL-17A production. *A*, Isolated splenocytes (1×10^5) from wild-type ($Tyk2^{+/+}$), $Tyk2^{+/-}$, or $Tyk2^{-/-}$ mice were analyzed for IL-2 production and proliferative responses after stimulation with or without Con A (0–10 μg/ml) for 48 h. Results are representative of two independent experiments. *B*, Isolated splenocytes (5×10^4) from $Tyk2^{+/+}$, $Tyk2^{+/-}$, or $Tyk2^{-/-}$ mice were analyzed for IFN-γ production after stimulation with or without IL-2 (0–3 ng/ml) in the presence of anti-CD3 mAb for 48 h. Results are representative of two independent experiments. *C*, Isolated splenocytes (5×10^4) from $Tyk2^{+/+}$, $Tyk2^{+/-}$, or $Tyk2^{-/-}$ mice were analyzed for IFN-γ production after stimulation with or without IL-12 (0–3 ng/ml) in the presence of anti-CD3 mAb for 48 h. Results are representative of two independent experiments. *D*, Isolated splenocytes (5×10^4) from B10.Q/Ai or B10.D1 mice were analyzed for IFN-γ production after stimulation with or without IL-12 (0–3 ng/ml) in the presence of anti-CD3 mAb for 48 h. Results are representative of two independent experiments.

Downloaded from http://jimmunol.org/ at Kyushu Univ 00A Noogakubu Tosho on May 21, 2012

of footpad swelling were taken at 24 h after challenge, using a thickness gauge (Mitutoyo, Kanagawa, Japan). The magnitude of the DTH responses was determined from differences in footpad thickness between the Ag-and saline-injected footpads.

IMQ treatment and scoring severity of skin inflammation

At 8–11 wk of age, mice received a daily topical dose of 5 mg commercially available IMQ cream (5%) (Beselna Cream; Mochida Pharmaceuticals, Tokyo, Japan) on a side of both ears for 6 consecutive days (29). To score the severity of inflammation of the ear skin, both affected ear thickness and ear tissue weight were measured. At the days indicated, the ear thickness of both ears was measured using the thickness gauge (Mitutoyo) and averaged. Also, after application on 4 consecutive days, ears were collected for quantitative PCR analysis, and ear-draining lymph node cells were collected for FACS analysis. In FACS analysis, cells were stimulated for 4 h by PMA/ionomycin with GolgiPlug and stained with anti-CD4 Ab conjugated with Alexa Fluor 647 (BD Pharmingen) and anti–IFN-γ or anti–IL-17 Ab, as indicated.

DSS-induced colitis

Colitis was induced by means of drinking water supplemented with 3% DSS (45,000–50,000 m.w.; MP Biomedicals, Santa Ana, CA), as described previously (30). Control mice were treated in a similar manner with drinking water without DSS. The disease activity index (DAI) and histological score were assessed in accordance with established criteria (30), which combined scores of weight loss, consistency, and bleeding divided by 3, and acute clinical symptoms with diarrhea and/or extremely bloody stools.

Hapten-induced colitis

TNBS-induced colitis has been described (31). Mice were immunized with 3.5 mg TNBS (Sigma-Aldrich) in 40% ethanol by intrarectal

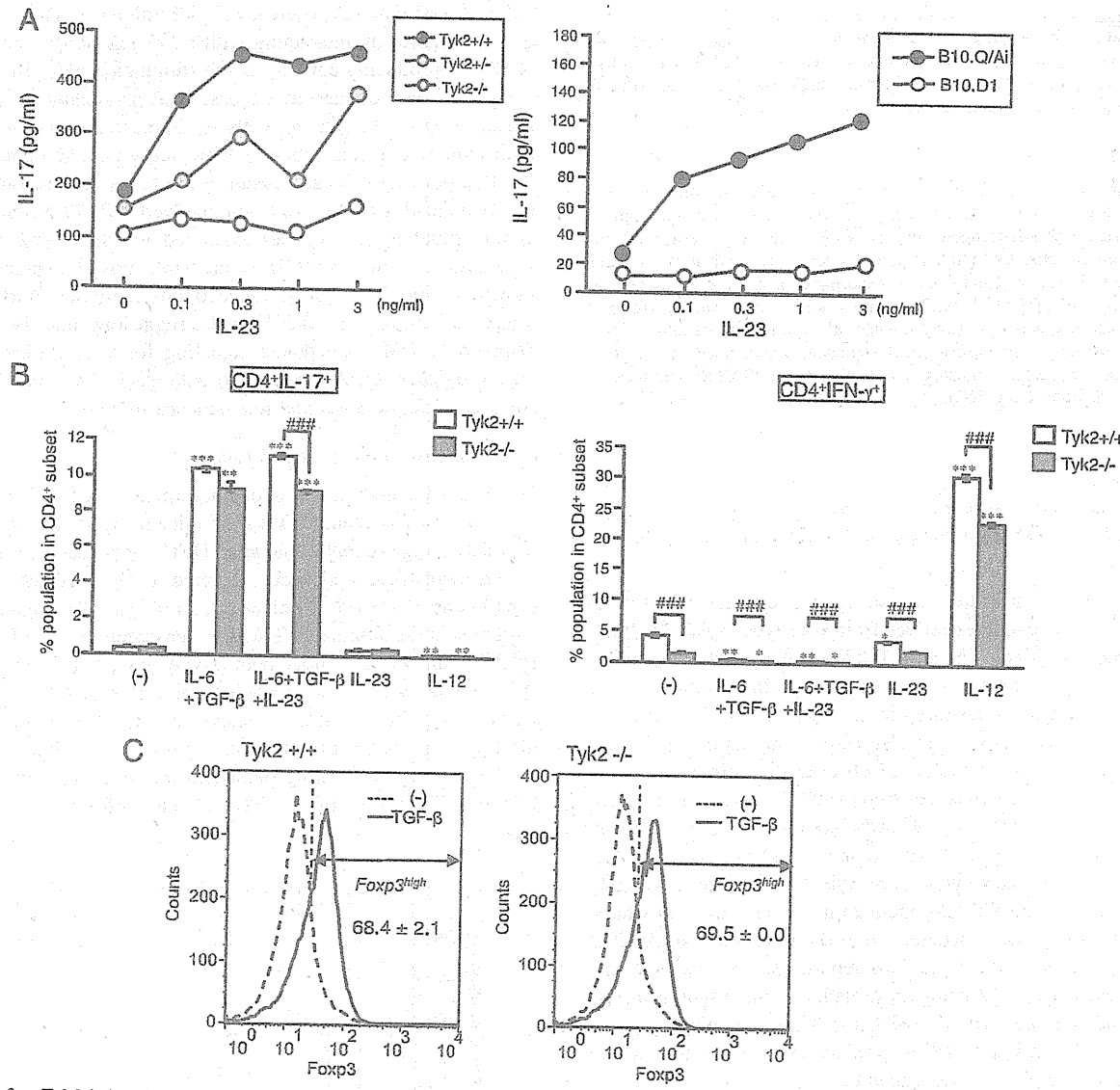

FIGURE 2. Tyk2 is involved in IL-23–induced IL-17A production and Th17 differentiation. *A*, Isolated splenocytes (2×10^5) from $Tyk2^{+/+}$, $Tyk2^{+/-}$, or $Tyk2^{-/-}$ mice were analyzed for IL-17 production after stimulation with or without IL-23 (0–3 ng/ml) in the presence of anti-CD3 mAb for 72 h. Results are representative of two independent experiments. Also, the same analysis was done using isolated splenocytes (5×10^4) from B10.Q/Ai or B10.D1 mice, and comparable results were observed. *B*, Isolated $CD4^+CD62L^+$ T cells (2.5×10^6) from $Tyk2^{+/+}$ or $Tyk2^{-/-}$ mice were stimulated with plate-bound anti-CD3 mAb (5 μg/ml) and soluble anti-CD28 mAb (1 μg/ml) in Th1/Th17 cell-inducing conditions. Seventy-two hours poststimulation, cells were harvested and immediately subjected to intracellular cytokine staining for IL-17 and IFN-γ. $IL\text{-}17^+$ and $IFN\text{-}\gamma^+$ cell populations were gated, and their ratios were compared. The results are mean ± SD of three independent experiments. *C*, Isolated $CD4^+CD62L^+$ T cells (2.5×10^6) from $Tyk2^{+/+}$ or $Tyk2^{-/-}$ mice were stimulated in the Treg-inducing conditions. Seventy-two hours poststimulation, cells were analyzed by Foxp3 staining. Representative graphs of three independent experiments are shown. Dashed line indicates the staining of naive T cells without TGF-β stimulation, and solid line indicates staining with TGF-β stimulation. Results were analyzed based on the percentage of $Foxp3^{high}$ population in $Tyk2^{+/+}$ or $Tyk2^{-/-}$ cells. The results represent mean ± SD. $^*p < 0.05$, $^{**}p < 0.01$, $^{***}p < 0.001$ compared with control group; $^{\#\#\#}p < 0.001$ compared with $Tyk2^{+/+}$ group.

Downloaded from http://jimmunol.org/ at Kyushu Univ 00A Noogakubu Tosho on May 21, 2012

administration. Each experimental group contained six 6–9-wk-old female mice.

Extraction of tissue RNA and TaqMan analysis of gene expression

RNA was extracted from ears and colons using ISOGEN (Nippon Gene, Tokyo, Japan). Using 5 μg total RNA template, cDNA was prepared using a High Capacity cDNA Reverse Transcription kit (Applied Biosystems, CA). Quantitative real-time PCR analyses of the respective gene, as well as the control GAPDH mRNA transcripts, were carried out using TaqMan Gene Expression assay probe/primer mixture and TaqMan Gene Expression Master Mix. PCR amplification and evaluation were performed using Applied Biosystems 7900HT Fast Real-Time PCR System. The reverse transcription and PCR conditions were in accordance with the manufacturer's instructions, and PCR was performed for 40 cycles.

Histology

Sections from formalin-fixed, paraffin-embedded ears were stained with H&E, and epidermal thickness was measured using a BIOREVO BZ-9000 microscope and measurement module BZ-H1ME (KEYENCE, Tokyo, Japan). Using this software, the epidermal thickness was measured at six positions per section and averaged.

Statistical analyses

All unpaired data were analyzed by an F test to evaluate the homogeneity of variance. If the variance was homogeneous, the Student *t* test was applied. If the variance was heterogeneous, the Welch *t* test was performed. For paired comparisons, the Student paired *t* test was performed. In other cases, the Wilcoxon rank-sum test, for scoring data, and the Tukey test, for the comparison of $Tyk2^{+/+}$, $Tyk2^{+/-}$, and $Tyk2^{-/-}$ mice, were performed. The log-rank test was performed in survival experiments. A value of $p < 0.05$ was chosen as an indication of statistical significance. A statistical comparison was performed using statistical software (SAS System Release 8.2; SAS Institute, Cary, NC).

Results

In vitro experiments reveal the involvement of Tyk2 in IL-12–induced IFN-γ production and IL-23–induced IL-17A production

To clarify and confirm the roles of Tyk2 in effector T cell functions, we used splenocytes derived from wild-type ($Tyk2^{+/+}$), Tyk2-heterodeficient ($Tyk2^{+/-}$), and Tyk2-deficient ($Tyk2^{-/-}$) mice. These three types of splenocytes exhibited similar responses to the T cell mitogen Con A, resulting in the production of IL-2 and cell growth (Fig. 1*A*). These cells also showed no significant differences in their IFN-γ production levels after IL-2 stimulation (Fig. 1*B*). However, the splenocytes from $Tyk2^{-/-}$ mice did not produce IFN-γ in response to IL-12, whereas those from $Tyk2^{+/+}$ and $Tyk2^{+/-}$ mice did (Fig. 1*C*). The impaired response to IL-12 was also observed in splenocytes from Tyk2-mutant mice (B10.D1) (Fig. 1*D*). Notably, the Tyk2-deficient mice used in this study have a BALB/c background, whereas B10.D1 mice have a C57BL/10SnSg background. In a previous report, we demonstrated unresponsiveness to IL-12 using Tyk2-deficient mice with a mixed background of 129/SV and C57BL/6 (8). Thus, the involvement of Tyk2 in IL-12–induced IFN-γ production is general and independent of the genetic background.

IL-12 and IL-23 are heterodimeric cytokines composed of a common p40 subunit and a p35 or p19 subunit, respectively. Unlike IL-12, IL-23 promotes a distinct $CD4^+$ T cell phenotype characterized by the production of IL-17, denoted Th17 cells (15). IL-23 enhances Th17 function and survival by acting on differentiated Th17 cells that express the IL-23R (15). Because the IL-12Rβ1 chain is also part of IL-23R and associates with Tyk2, we examined the effect of Tyk2 on IL-23–induced IL-17A production. As shown in Fig. 2*A*, IL-23–mediated stimuli induced IL-17 production in the splenocytes from $Tyk2^{+/+}$ and B10.Q/Ai control mice in dose-dependent manners. The splenocytes from $Tyk2^{-/-}$ and B10.D1 mice completely failed to produce IL-17 in response to IL-23–mediated stimuli. Notably, the splenocytes from $Tyk2^{+/-}$ mice exhibited a moderate decrease in IL-17 production after stimulation with all of the tested concentrations of IL-23. Therefore, IL-23–induced IL-17 production is strongly dependent on the Tyk2 protein context and is distinct from the effects of Tyk2 on IL-12–induced IFN-γ production. To further examine the involvement of Tyk2 in Th17 differentiation, we cultured $CD4^+CD62L^+$ naive T cells in the presence of TGF-β and IL-6. The cultures of $Tyk2^{+/+}$ cells contained significantly higher proportions of IL-17–producing cells than did those of $Tyk2^{-/-}$ cells, although both cultures induced IL-17–producing cells (Fig. 2*B*). The subsequent addition of IL-23 increased the numbers of IL-17–producing cells in the $Tyk2^{+/+}$ cell cultures but not in the $Tyk2^{-/-}$ cell cultures. Therefore, Tyk2 influences Th17 induction or maintenance by interacting with IL-23 signaling. The number of IFN-γ–producing cells by IL-12 stimulation was also affected in $Tyk2^{-/-}$ cell culture, as we described previously (8). We also examined IL-10–producing cells by intracellular staining in the same situation (data not shown). However, we could not detect any IL-10–producing cells as a result of the lower expression level of IL-10, indicating that IL-10 is not involved in Th17 differentiation in this situation. We further examined whether Tyk2 regulates Treg differentiation by TGF-β–mediated Foxp3 expression. As shown in Fig. 2*C*, TGF-β–induced differentiation into $Foxp3^+$ Tregs was normal in $Tyk2^{-/-}$ cells, suggesting that Tyk2 is not involved in TGF-β–mediated signaling for Treg differentiation. Taken together, Tyk2 is related to pathogenic Th1 and Th17 but not Treg differentiation and maintenance in vivo.

DTH responses in Tyk2-deficient mice

The data obtained in the above-described in vitro experiments encouraged us to examine $Tyk2^{-/-}$ mice using IL-12– and/or IL-23–related experimental models. DTH responses are strongly T cell dependent and were reported to be defective in IL-12p40– and IL-23p19–deficient mice (28, 32). To evaluate DTH responses in the absence of Tyk2, we sensitized groups of $Tyk2^{+/+}$, $Tyk2^{+/-}$, and $Tyk2^{-/-}$ mice with mBSA in CFA and then elicited DTH responses after 7 d by injection of mBSA or saline (negative control) into the footpad. As shown in Fig. 3, specific footpad swelling was observed in the three types of mBSA-injected mice, but the degrees of swelling paralleled the levels of Tyk2 protein ($83.9 \pm 9.1 \times 10^{-2}$ mm for $Tyk2^{+/+}$ mice, $46.0 \pm 30.5 \times 10^{-2}$

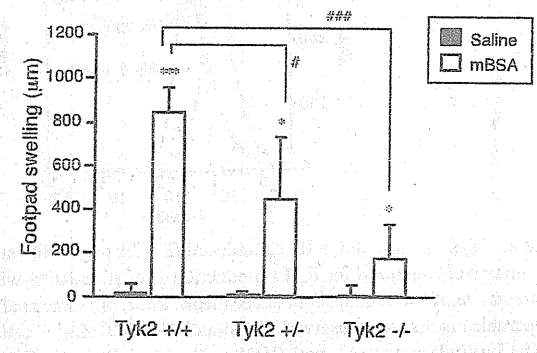

FIGURE 3. DTH responses in Tyk2-deficient mice. Mice immunized with mBSA were induced DTH reaction by the Ag injection into left heel. Ag-specific swelling 24 h after challenge was calculated as footpad thickness over the value measured just before the challenge. The results were averaged over all five mice in each group; error bars represent SDs. $^*p < 0.05$, $^{***}p < 0.001$ compared with saline-treated group; $^{\#}p < 0.05$, $^{\#\#\#}p < 0.001$ compared with $Tyk2^{+/+}$ mice.

Downloaded from http://jimmunol.org/ at Kyushu Univ 00A Noogakubu Tosho on May 21, 2012